Cluster Science with SZE and Multi-wavelength Observations

Keiichi Umetsu (梅津敬一), ASIAA

In collaboration with J. Sayers, S. Golwala, N. Czakon, T. Mroczkowski, B. Mason, M. Sereno, S.M. Molnar, N. Okabe, T. Broadhurst, E. Medezinski, A. Zitrin, M. Nonino, M. Donahue, M. Postman, et al.

Importance of Multi-wavelength, Multi-probe Cluster Studies

http://www.mpa-garching.mpg.de/galform/data_vis/

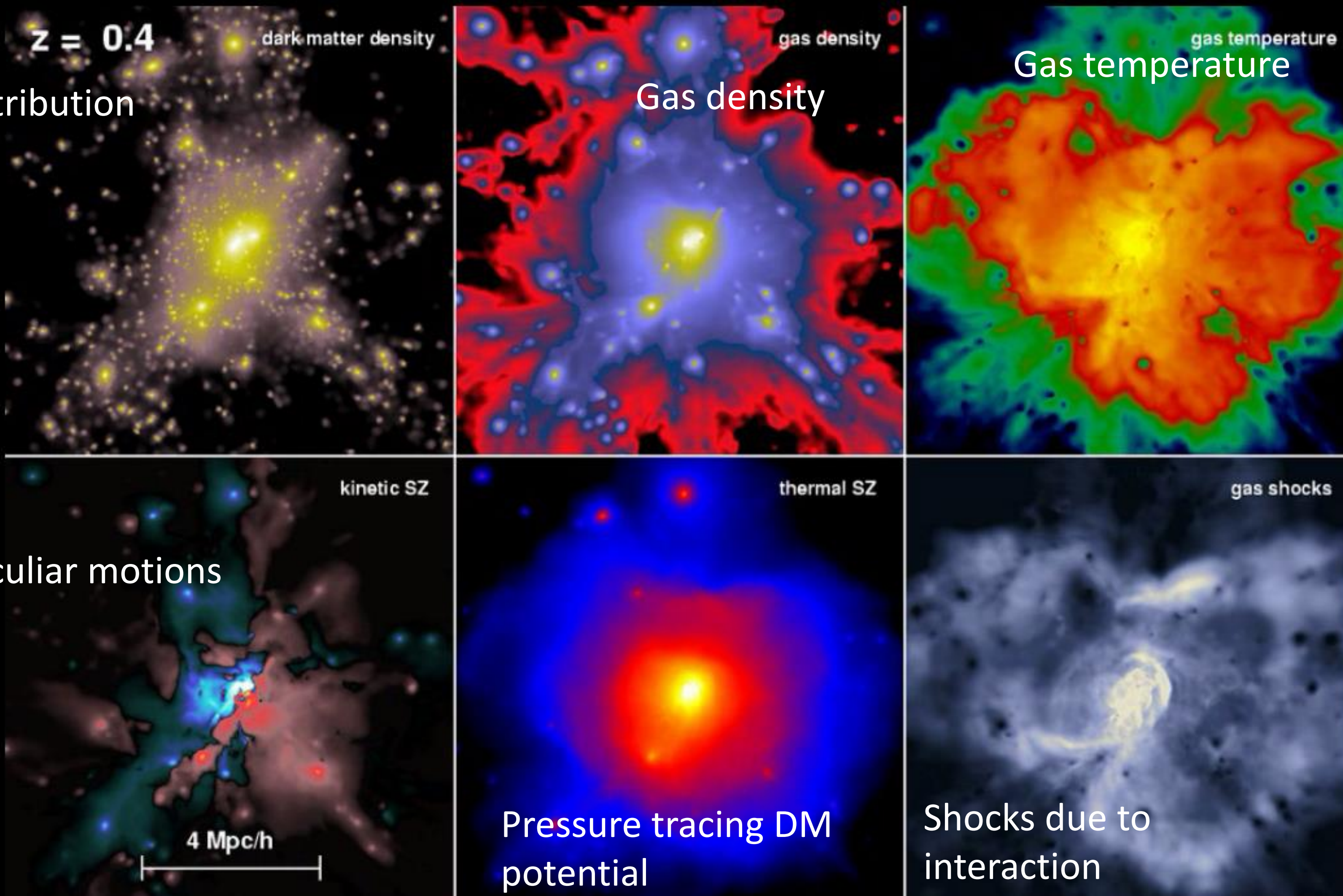

Contents

1. Cluster Peculiar Velocities from kSZE and Moving-lens-effect Measurements
2. Mass, Shape, and Thermal Properties of Clusters from SZ+Xray+Lensing Data
3. Ensemble-averaged Pressure vs. Mass Profiles from Stacked SZE and Lensing Analyses

(1) Cluster Peculiar Velocities from kSZE and Moving-Lens Effect (Lensing-analog of the Rees-Sciama Effect) Measurements

MACS0717: Complex Merging Cluster at z=0.55 (a pink elephant?)

Multiple cores revealed by optical imaging/spectrcoospy, X-ray, and SL data

SUBARU WL mass map (Medezinski, Umetsu+13)

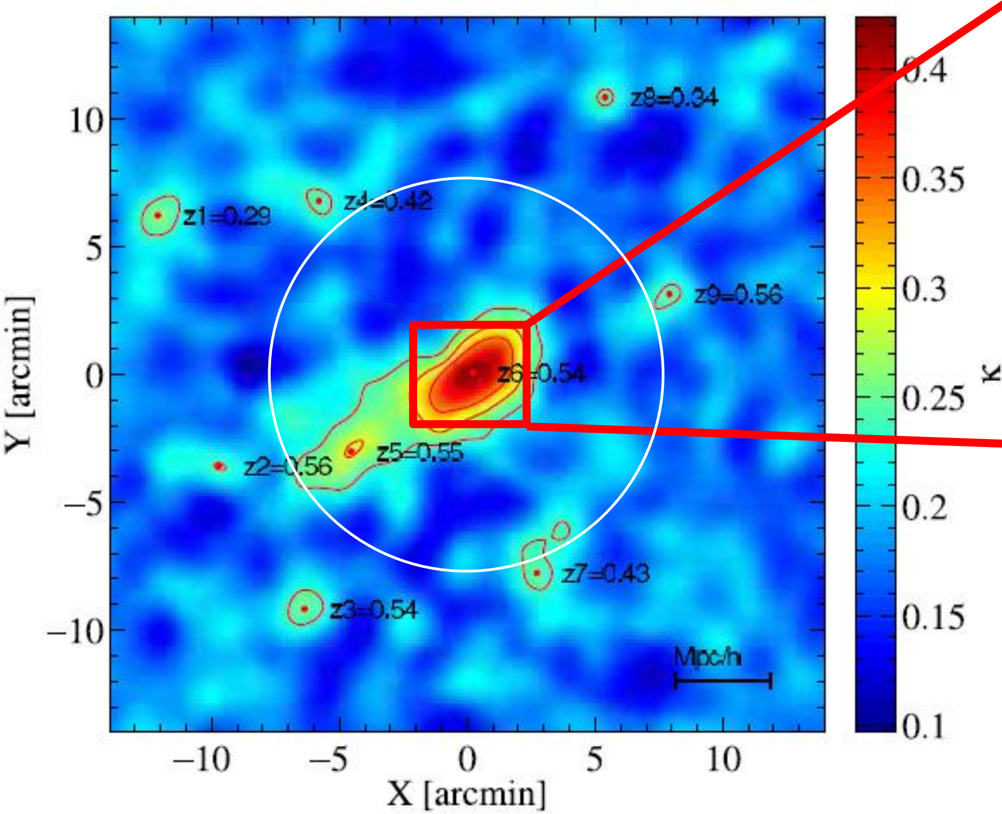

Circle: R_{vir}=2Mpc/h (7.5 acmin)

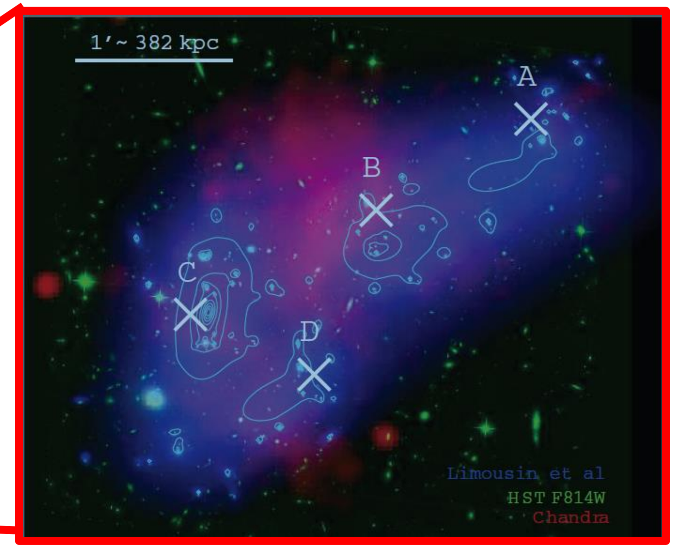

- Lensing-selected CLASH cluster (one of the HST-FF clusters)
- Largest known Einstein radius, R_E=60”
- @z=3 (Zitrin+09)
- Multiple clumps with high relative velocities (Ma+09; Mroczkowski+12)
- Most massive cluster known at z>0.5 (Medezinski, KU+13): $M_{vir}=3\times10^{15}\ M_{sun}$

HST Weak vs. Strong Lensing Analysis

Nonparametric HST-WL mass reconstruction with Umetsu+Broadhurst08 MEM method

Parametric HST-SL mass reconstruction with Light-Traces-Mass (LTM) Zitrin+09 method

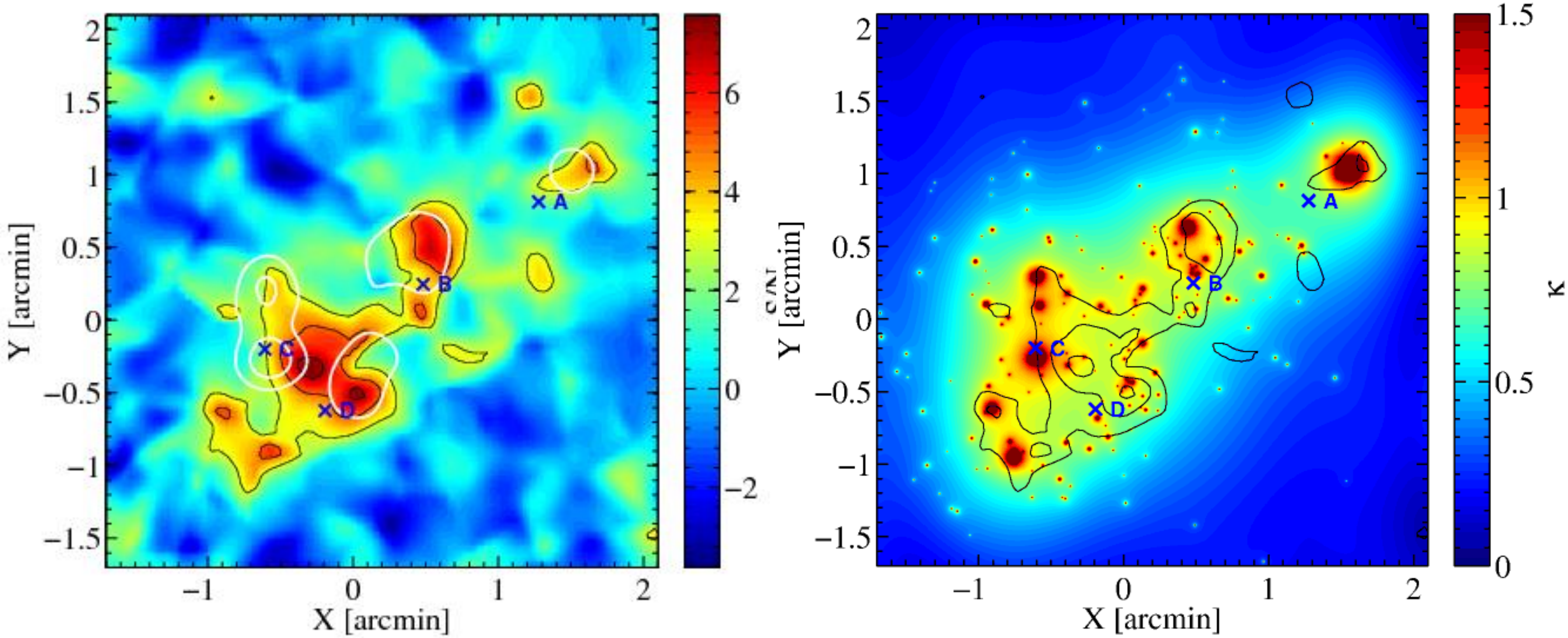

Overall, the galaxies trace the lensing mass distribution.
Deeper HST-FF imaging will improve WL constraints on the possible DM-galaxy offsets.

Medezinski, Umetsu+CLASH 2013, ApJ, 777, 43

kSZE detection in an individual cluster

Sayers, Mroczkowski, … Umetsu 2013, ApJ, 778, 52

Multi-halo modeling with BOLOCAM/CSO multi-freq SZE (140 & 268 GHz) and Chandra X-ray observations

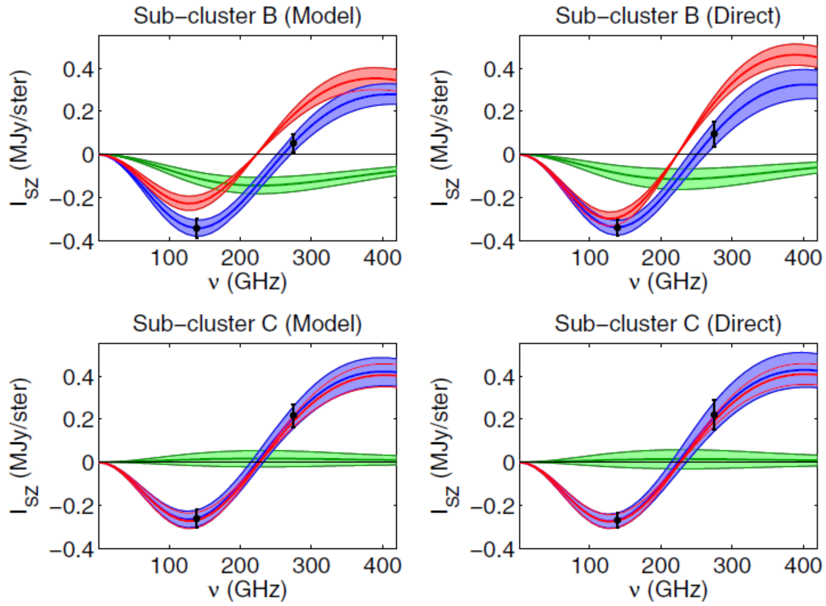

Red: tSZE **Green**: kSZE **Blue**: total

B: V_{opt}=+3200+/-250km/s, **V_{kSZ}=+3500+/-900 km/s**
C: V_{opt}= -730+/-490km/s, **V_{kSZ}= -550+/-1400 km/s**

Significant kSZE signal toward B (4.2 sigma)

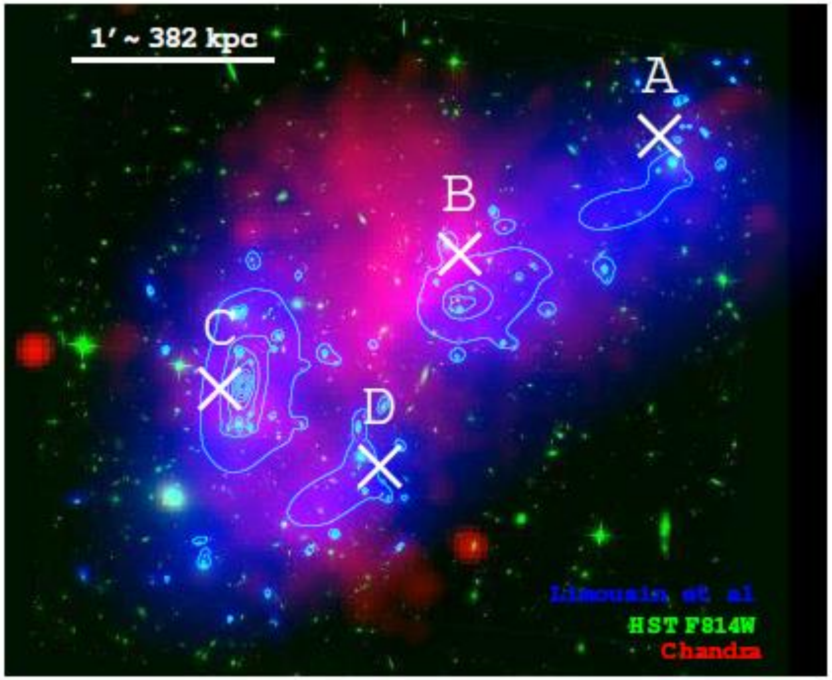

FIG. 1.— False-color composite image of MACS J0717.5+3745 with the lensing results of Limousin et al. (2012) in blue, the Hubble Space Telescope image using the F814W filter in green, and the *Chandra* X-ray image in red. The blue contours show the Limousin et al. (2012) result on a linear scale, and clearly indicate the four sub-clusters labeled A through D, with white Xs marking the sub-cluster positions determined by Ma et al. (2009) from the galaxy distribution.

Moving Lens (Birkinshaw-Gull) Effect

Lensing-analog of the Rees-Schiama effect

$$\left(\frac{\Delta\nu}{\nu}\right) = -2\int \dot{\Phi}\, dt$$

Change of potential along photon path due to lens motion

$$\left(\frac{\Delta\nu}{\nu}\right)_{BG} = -2\int \mathbf{v}_{\perp}\cdot\nabla_{\perp}\Phi\, dt \approx \mathbf{v}_{\perp}\cdot\hat{\boldsymbol{\alpha}}$$

Observable pairwise frequency shift between multiply-lensed images

$$\left(\frac{\Delta\nu}{\nu}\right)_{\rm pair} \approx 2v_{\perp}\theta_E = 2\times10^{-6}\left(\frac{v_{\perp}}{2000{\rm km/s}}\right)\left(\frac{\theta_E}{30''}\right)$$

~ (sub) 1km/s velocity shift

Simulated DM flow centered on the Bullet

$$\left(\frac{\Delta \nu}{\nu}\right)_{BG} = \mathbf{v}_{\perp} \cdot \hat{\boldsymbol{\alpha}}$$

AMR FLASH (DM+gas) simulation of the Bullet Cluster

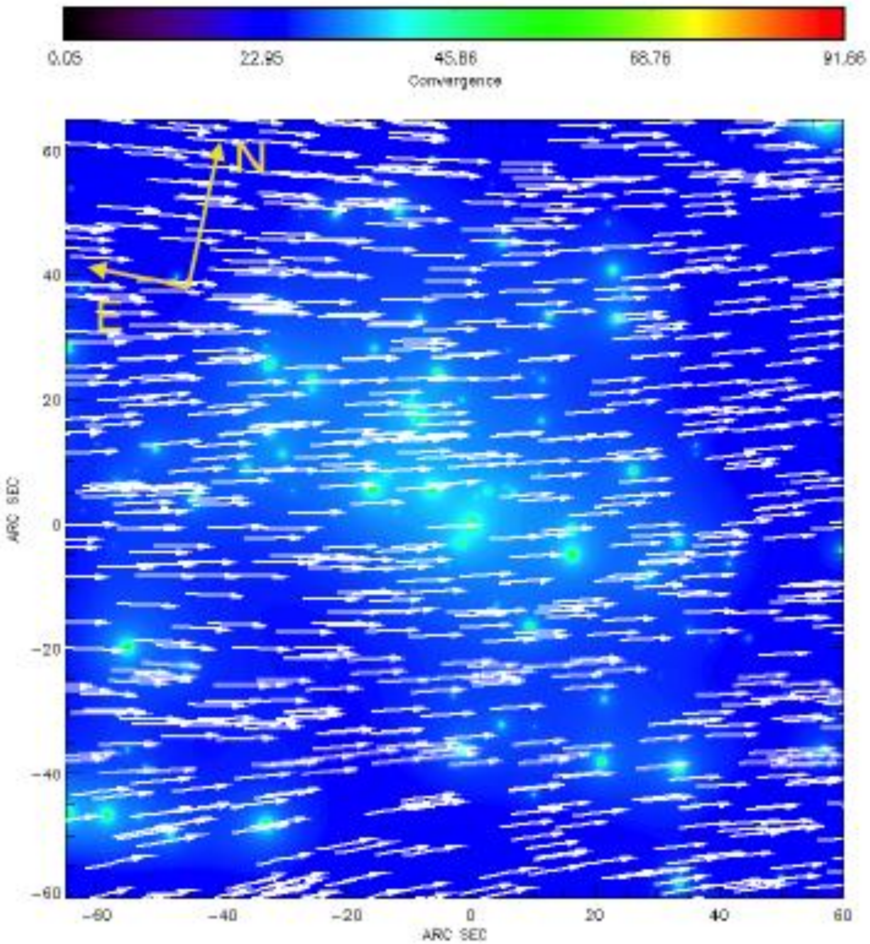

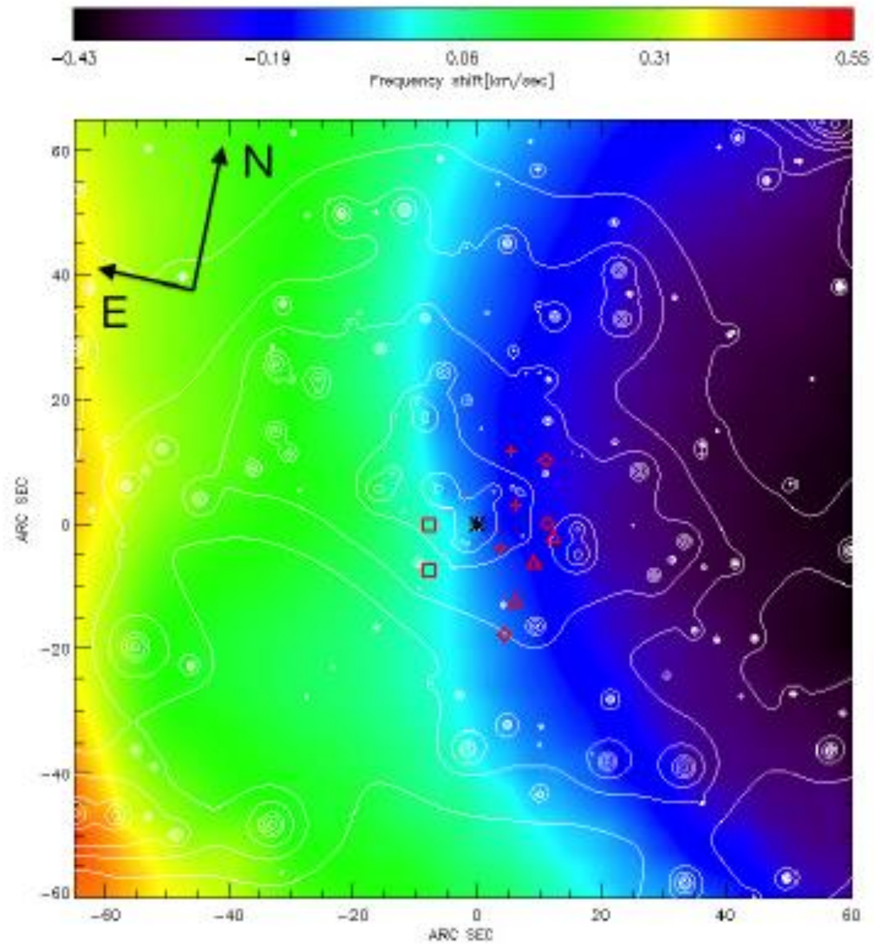

Molnar, Broadhurst, Umetsu+13, ApJ, 774, 70

(2) Mass, Shape, and Thermal Properties of Galaxy Clusters from Multi-probe Observations

WL vs. tSZE Complementarity

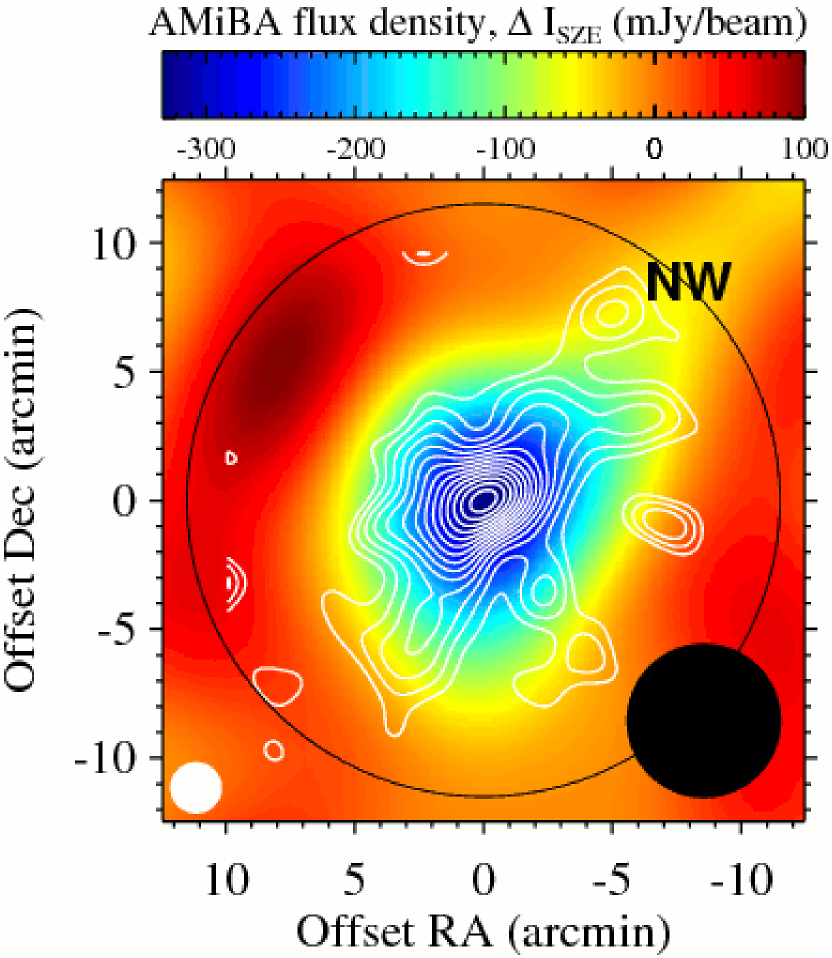

Lensing convergence:

$$\kappa = \int dl\, \Sigma_{\rm crit}^{-1}(\rho_m - \langle \rho_m \rangle) \propto \int \rho_m dl$$

Comptonization parameter:

$$y = \int d\tau_e \frac{k_B(T_e - T_\gamma)}{m_e c^2} \approx \frac{\sigma_T}{m_e c^2} \int P_e dl \propto \int f_{\rm gas} T_e \rho_m dl$$

- **Large scale**: gravitational potential
- **Small scale**: DM-gas deviations and non-equilibrium feature

Cold-front cluster A2142 @ z=0.09 from Ho+09

See also Okabe+Umetsu08; Umetsu+09; Munari+13

DM vs. ICM structure in an X-ray-selected relaxed cluster

$$\varepsilon_a = \sqrt{1-(a/c)^2}$$
$$\varepsilon_b = \sqrt{1-(b/c)^2}$$

HSE gas follows potential that is rounder than matter density (X-ray shape theorem by Buote & Canizares 94): $\varepsilon_{ICM} \sim 0.7\, \varepsilon_{DM}$ (Lee & Suto 03)

Relaxed CLASH cluster: MACS1206 at z=0.44 (Umetsu+12, ApJ, 755, 56)

SL+WL mass map from HST+SUBARU data

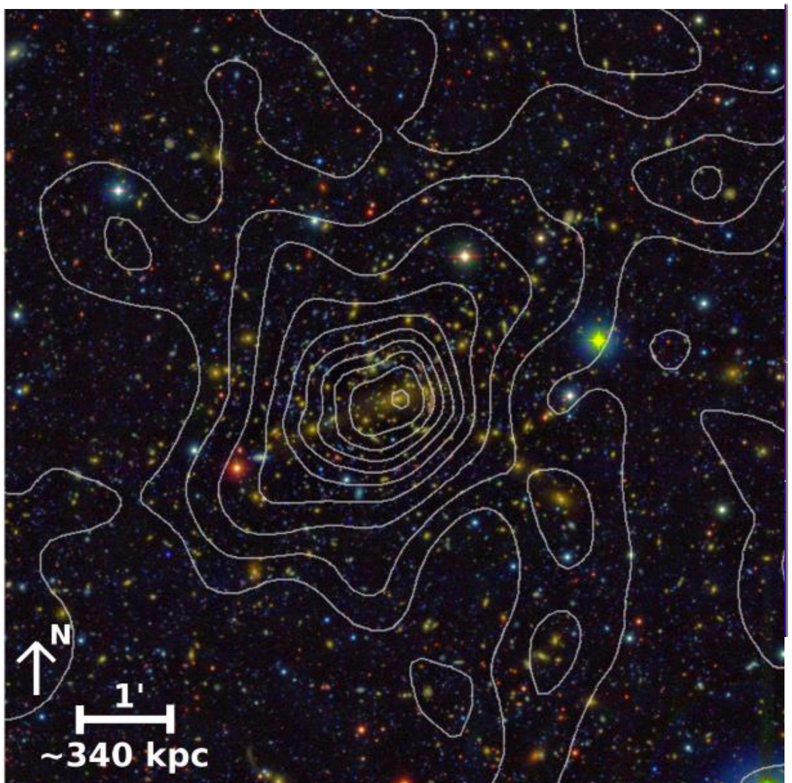

tSZE map from Bolocam@150GHz data

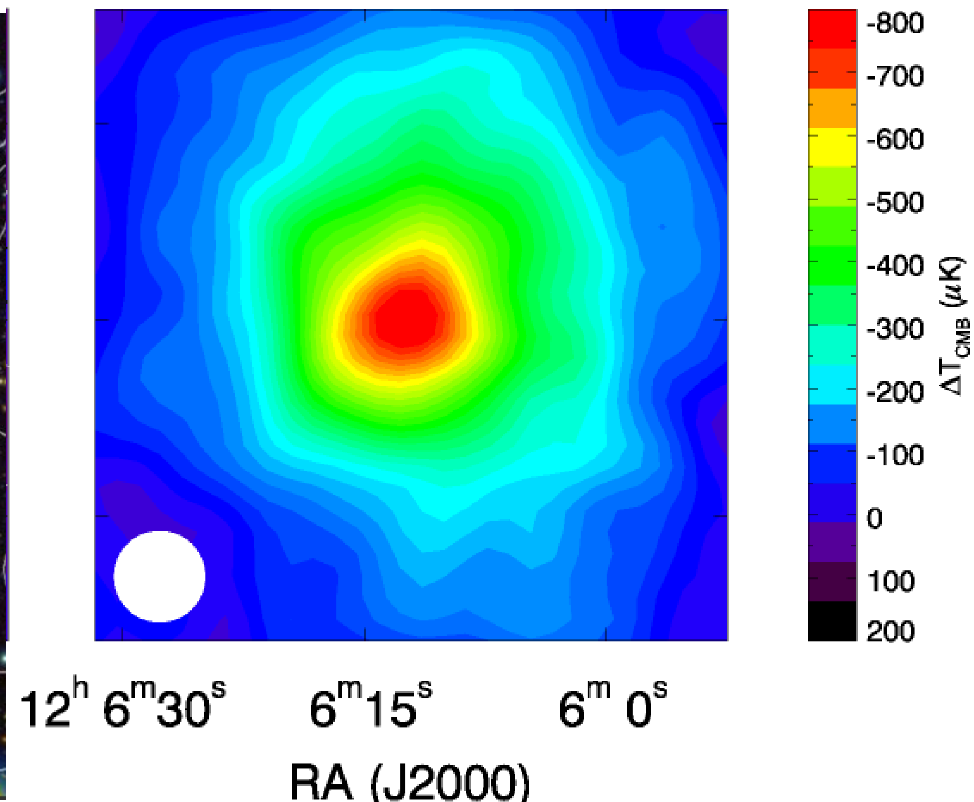

DM vs. ICM structure in an X-ray-selected relaxed cluster (contd)

- For MACS1206, lensing, X-ray-HSE, and SZE-HSE *spherical* mass estimates ($>r_{2500}$) agree (Umetsu+12).
- Biviano+CLASH (2013) showed that the pseudo phase-space density ρ/σ_v^3 of member galaxies follow power-law $r^{-1.9}$ (Taylor & Navarro 01).
- Indicating that MACS1206 **is close to HSE** AND **effectively spherical**: **line-of-sight sizescale ~ geometric-mean sizescale in projection space**

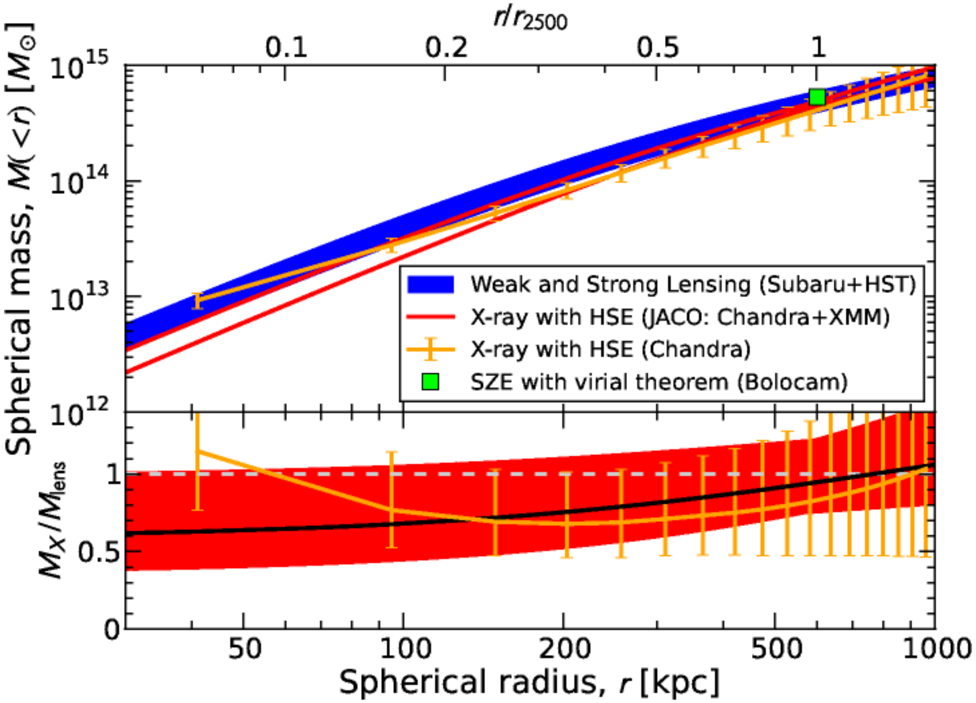

Umetsu+12

Triaxiality and Projection Effects

$$\Sigma_m = \int \rho_m dl \propto \left(l_\perp f_{\rm geo}\right)_{\rm matter}$$

$$\Sigma_g = \int \rho_g dl \propto \left(l_\perp f_{\rm geo}\right)_{\rm gas}$$

$$f_{\rm geo} \equiv \frac{\sqrt{e_P}}{e_\Delta} = \frac{l_{\rm los}}{l_\perp}$$

Projected density measurements scale with the ratio of LOS-to-projected sizescale

$$l_\perp = \frac{l_P}{\sqrt{e_P}}:$$

Geometric-mean sizescale in projection

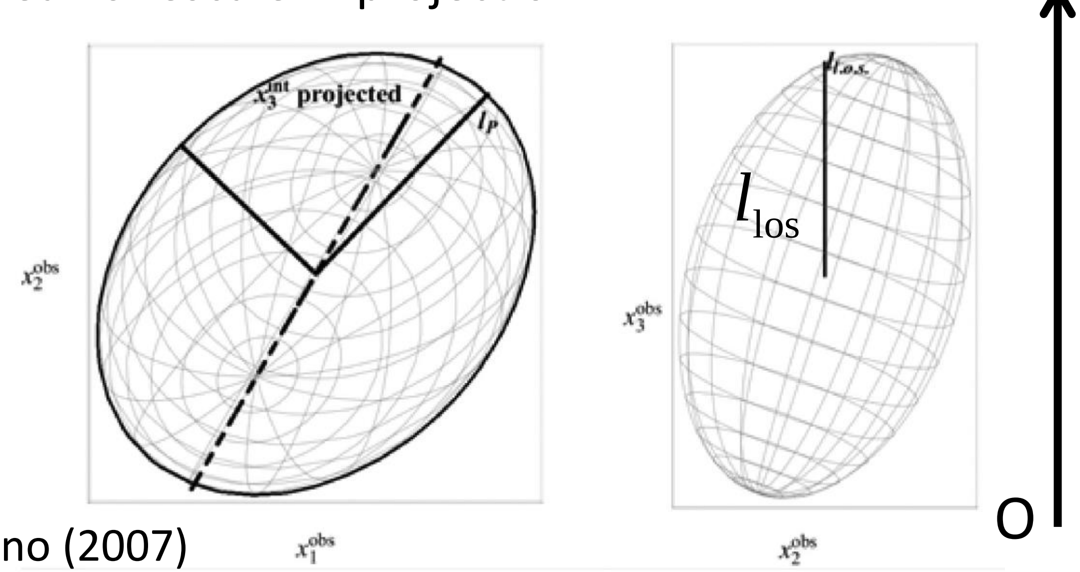

See Sereno & Umetsu (2011);
Stark (1977); Oguri et al. (2003); Sereno (2007)

DM vs. ICM structure in a strong-lensing cluster

Non-HSE gas follows matter density, rather than potential: $\varepsilon_{ICM} \sim \varepsilon_{DM}$

Strong lensing cluster: A1689 at z=0.18 (Umetsu & Broadhurst 08)

SDSS-defined cluster members (Kawaharada, Okabe+KU+10)

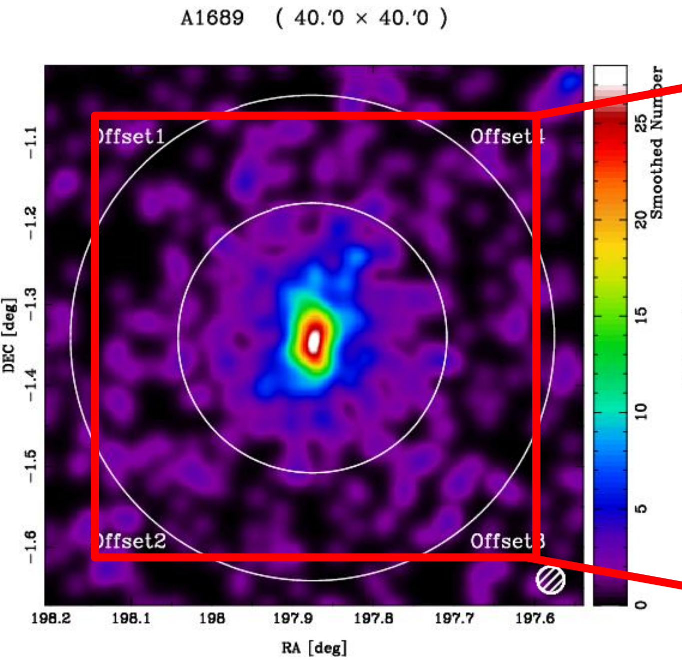

WL-mass map from Subaru (KU, Sereno+14, in prep)

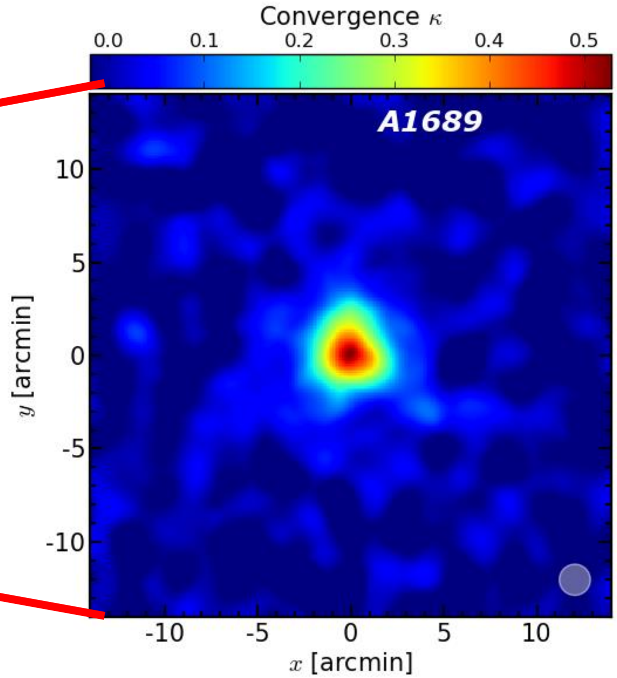

X-ray brightness from Chandra (Sereno+12)

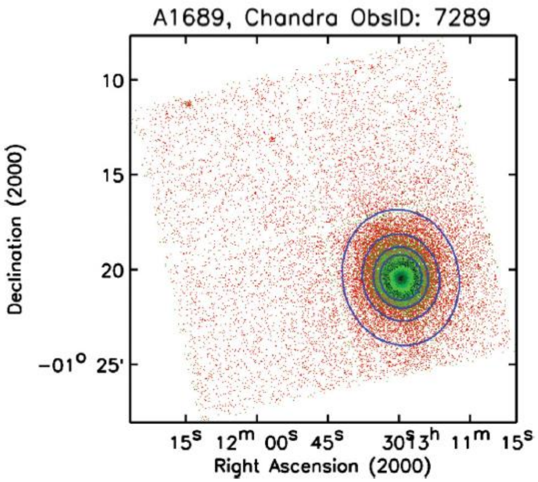

Figure 1. Exposure-corrected image of one of the *Chandra* observations

Discrepant HSE and Lensing Masses?

SUZAKU HSE vs. lensing M_{3D}(<r) of A1689 (Kawaharada, Okabe, Umetsu+10)

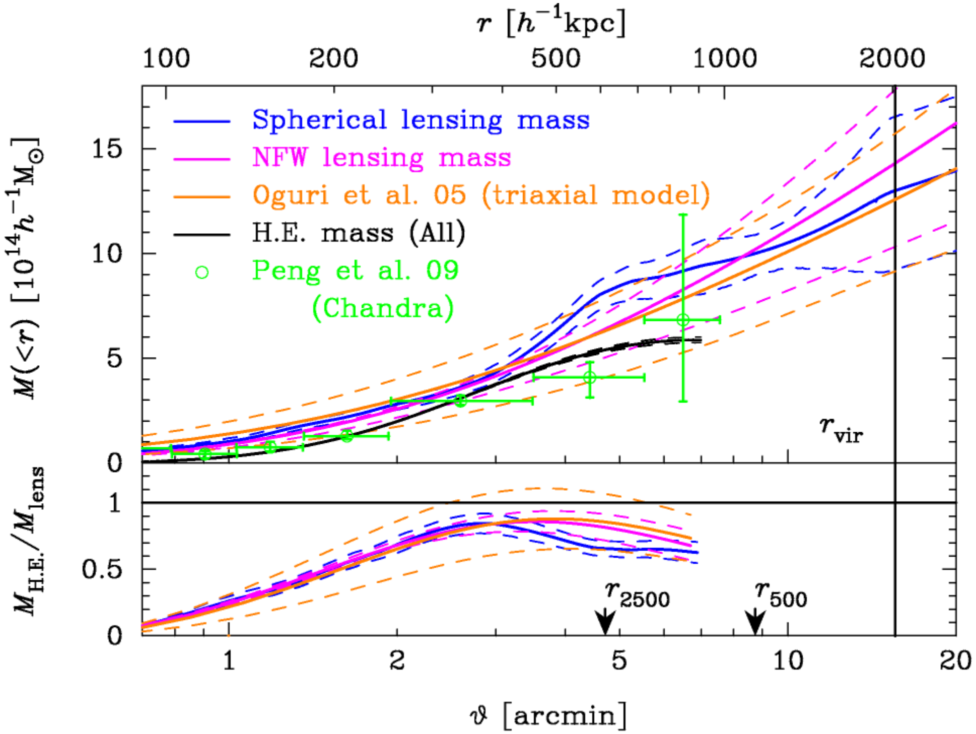

Marginalizing over intrinsic triaxial shape parameters increases the lensing errors in $M_{3D}(r)$, reflecting the lack of line-of-sight information (Oguri, Takada, Umetsu, Broadhurst 05).

M_{200c}= 1.3 (+0.2, -0.2) 10^{15} M_{sun}/h, c_{200c}=9.0 (+1.5, -1.5) by Umetsu & Broadhurst 08 NFW
M_{200c}= 0.9 (+0.1, -0.1) 10^{15} M_{sun}/h, c_{200c}=6.6 (+0.4, -0.4) by Peng+09 NFW
M_{200c}= 1.1 (+0.3, -0.5) 10^{15} M_{sun}/h, c_{200c}=14 (+2, -11) by Oguri+05 triaxial-NFW

Multi-probe approach for constraining 3D cluster structure

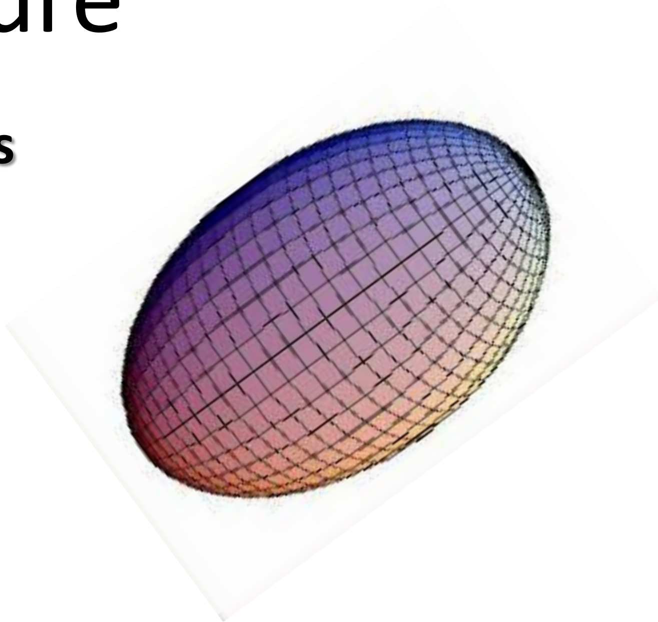

Combining lensing, X-ray, and tSZE observations

- **Strong-lensing**
  - inner matter density profile
  - 2D matter morphology
- **Weak-lensing**
  - outer matter density profile
  - 2D matter morphology (noisy)
- **X-ray**
  - emission-measure ($n_e^2 T^{1/2}$) and spec-temperature profiles
  - 2D gas morphology
- **tSZE**
  - thermal pressure profile out to ~r500
  - 2D gas morphology (challenging?: contamination, transfer function, ..)

$$\frac{(r_c)_\perp}{(r_c)_{\rm los}} \propto D_L \frac{S_X}{\Delta T_{\rm tSZE}} \frac{T_e^2}{\Lambda_X}$$

tSZE+X-ray constraining ICM sizescales both along **LOS** and in **projection**!!

Methodology

Total matter ICM

$$L(\mathbf{p}) = \underbrace{L_{\mathrm{WL}}(\mathbf{p}) L_{\mathrm{SL}}(\mathbf{p})}_{\text{Total matter}} \times \underbrace{L_{T_X}(\mathbf{p}) L_{S_X}(\mathbf{p}) L_{\mathrm{SZ}}(\mathbf{p})}_{\text{ICM}}$$

- **Morandi method** (Morandi, Limousin, Rephaeli, Umetsu+11; Morandi+12)
  - Total matter
    - triaxial generalization of NFW
  - ICM
    - $P_{tot} = P_{th} + P_{nth}$ follows gravitational potential, with $P_{nth}(R)/ P_{tot}(R) = \xi (R/R_{200})^n$
    - Small-eccentricity approximation for gravitational potential (Lee & Suto 03)
  - Couple total-matter and ICM distributions by using generalized HSE
- **Sereno method** (Sereno & Umetsu 11; Sereno, Ettori, Umetsu+13)
  - Total matter
    - Triaxial generalization of NFW
  - ICM
    - Triaxial matter and ICM halos coaligned with the same degree of triaxiality , T=(ε_b/ε_a)^2 < 1
  - Couple total-matter and ICM distributions by much less informative priors on geometric shape, without making equilibrium assumptions

Applications to A1689 (z=0.18)

Revisiting multi-probe analysis of A1689 with new WL (Subaru BVRIz) and tSZE (SZA/BIMA/OVRO) observations: Umetsu, Sereno+14 in prep.

- **WL**: 2D mass reconstruction from Subaru 2D-shear + magnification (KU)
- **SL**: 2D mass reconstruction from HST/ACS/WFC3 data (Sereno)
- **X-ray**: 2D morphology and brightness profile from Chandra@R<1200kpc (Ettori)
- **X-ray**: temperature profile from XMM data@R<900kpc (Ettori)
- **tSZE**: joint Y(R) modeling of BIMA+OVR+SZA data (Mroczkowski)

2D strong lensing (HST/ACS)

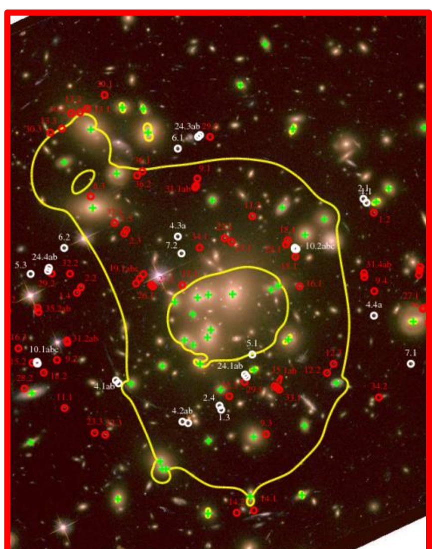

2D WL shear + magnif (Subaru)

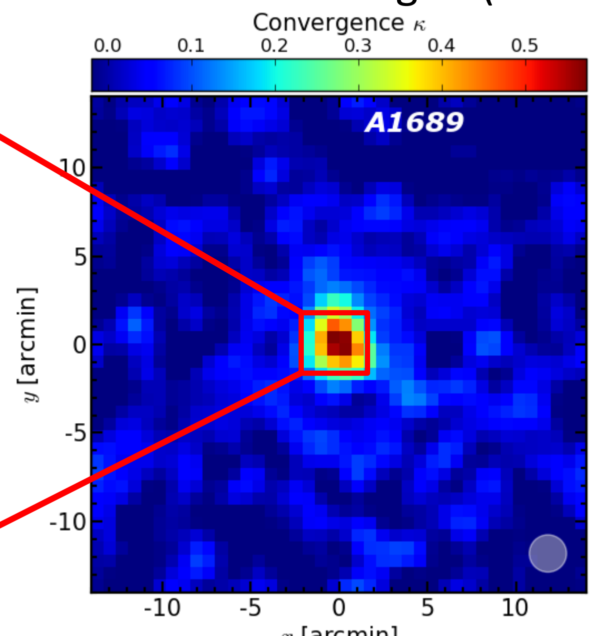

2D X-ray (Chandra/XMM)

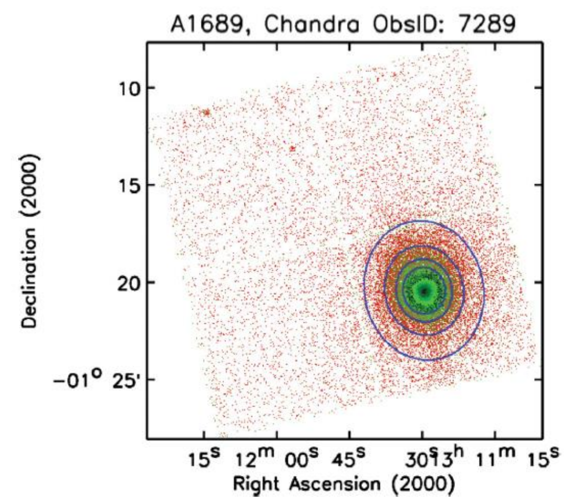

Figure 1. Exposure-corrected image of one of the *Chandra* observations

Joint Bayesian analysis of WL_{2D}+SL_{2D}+$Xray_{2D}$+SZE observations [Sereno+13 method]

- **Spherical NFW mass model** (WL-2D alone)
  - M_{200c}= (1.3 +/- 0.2) 10^{15} M_{sun}/h, c_{200c}=9.0 +/- 1.5
- **Triaxial NFW mass model** (w/o informative prior)
  - M_{200c}=(1.0 +/- 0.2) $10^{15}M_{sun}$/h, c_{200c}=6.2 +/- 0.8
  - a/c=0.45 +/- 0.16, b/c=0.57 +/- 0.17, cosθ=0.94 +/-
- **Including N-body priors on axis-ratio distribution**
  - M_{200c}=(1.0 +/- 0.2) $10^{15}M_{sun}$/h, c_{200c}=5.9 +/- 0.7
  - a/c=0.43 +/- 0.08, b/c=0.54 +/- 0.10, cosθ=0.95 +/- 0.04

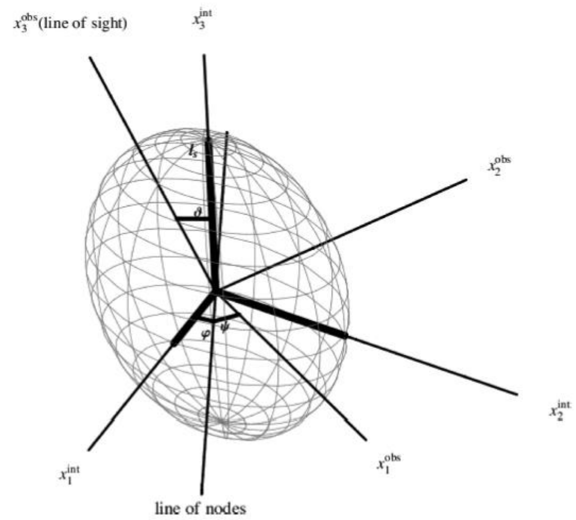

- **Results**
  - Insensitive to priors thanks to the improved WL/SZE data!
  - C_{200c} = 5-6 @ M_{200c}~$10^{15}M_{sun}$/h, compared to <c_{200c}>=3.3 +/- 1.1 by Bhattacharya+13 DM-only predictions
  - Similar matter and ICM eccentricities: e_{ICM} ~ 0.9 e_{DM}
  - Consistent with prolate structure with a/c~b/c~0.5
  - The semi-major axis is closely aligned with LOS: θ ~ 20 (+5, -10,) deg

Reconstructed $f_{gas}=M_{gas}/M_{tot}$

f_{gas} ~ 10% at r=1Mpc from multi-probe triaxial analysis

Umetsu, Sereno+14 (WL+SL+Xray+SZE)

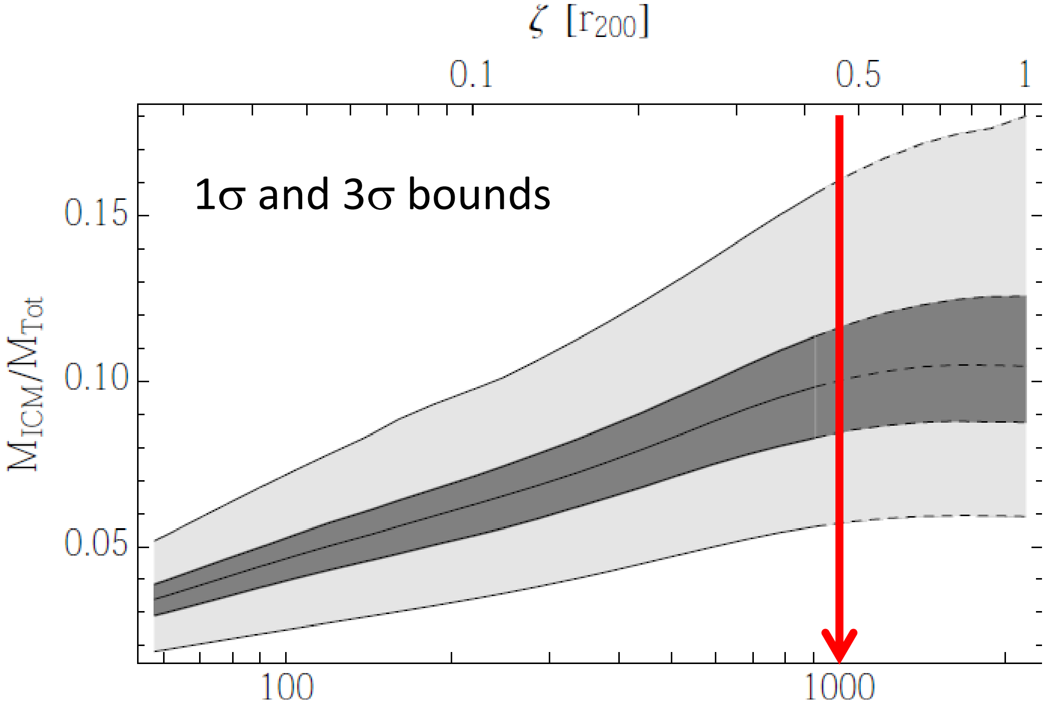

Kawaharada, Okabe, KU+10

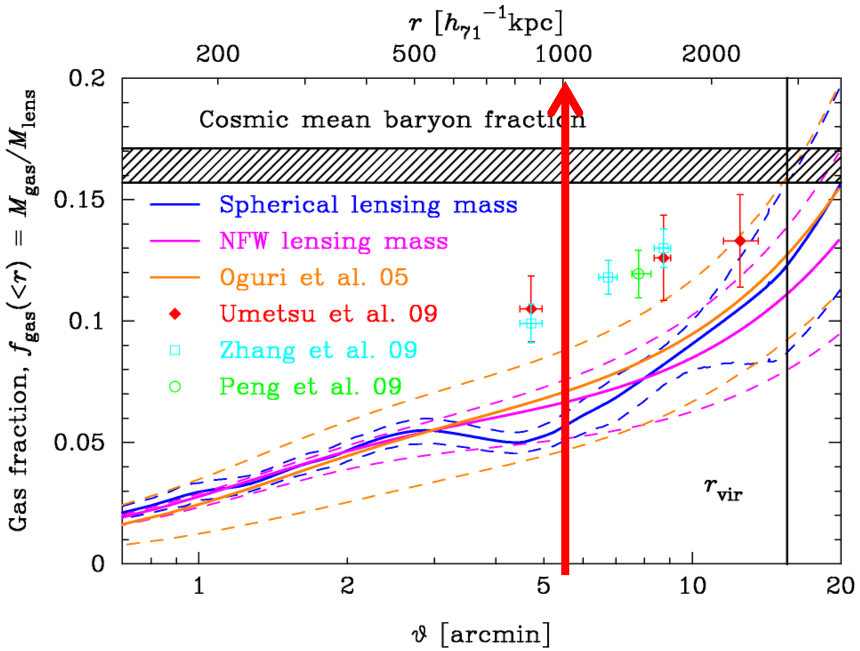

Reconstructed P_{th}/P_{tot}

- Approximately 20% nonthermal pressure support at r=50-1000kpc.
- The observed P_{th}/P_{tot} is more consistent with those found for $10^{15}M_{sun}$ clusters in AMR simulations of Molnar+10 with resolved subsonic gas motions.

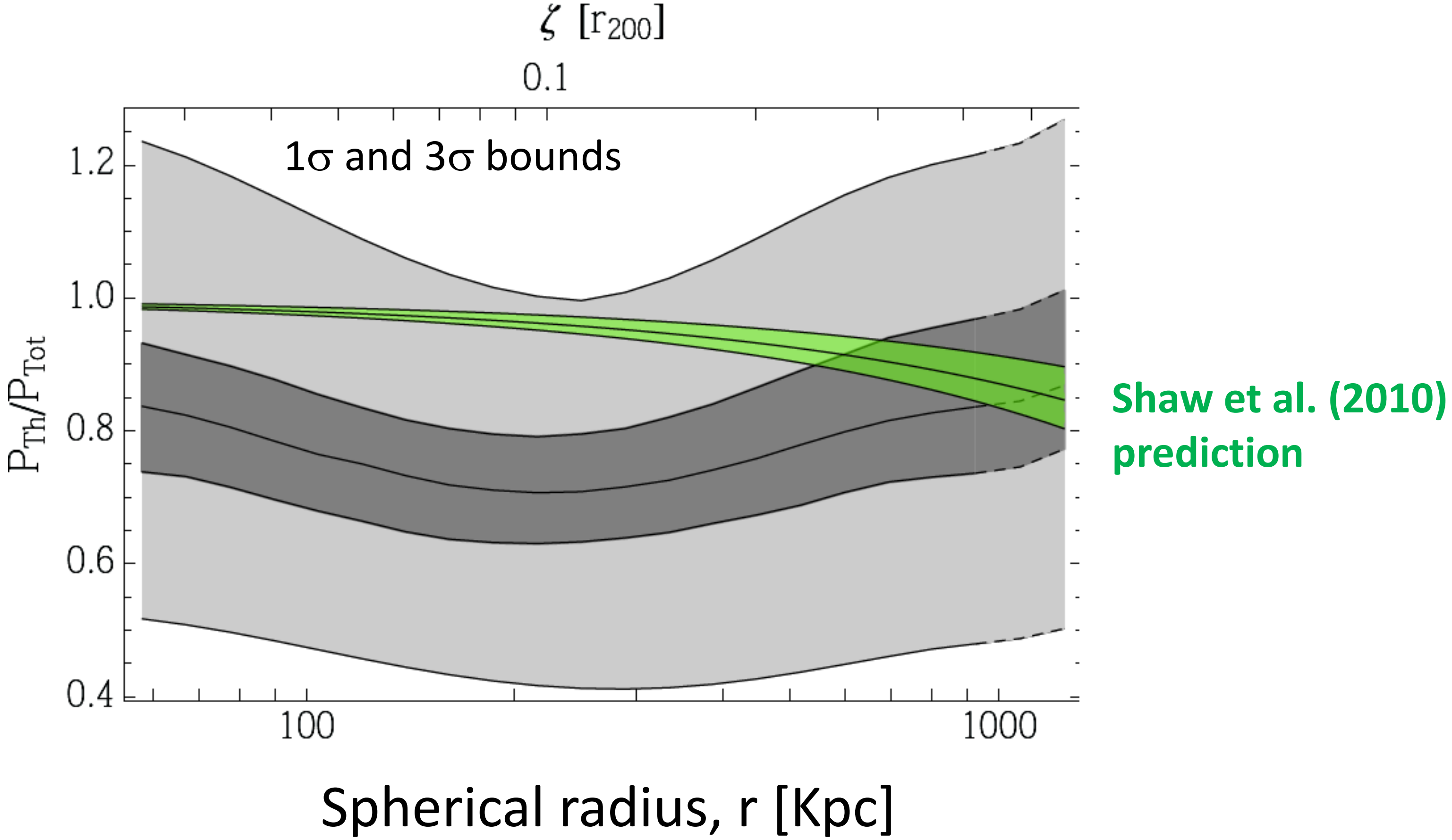

Future prospects / ongoing projects

BOXSZ sample of 45 clusters (Sayers+13)

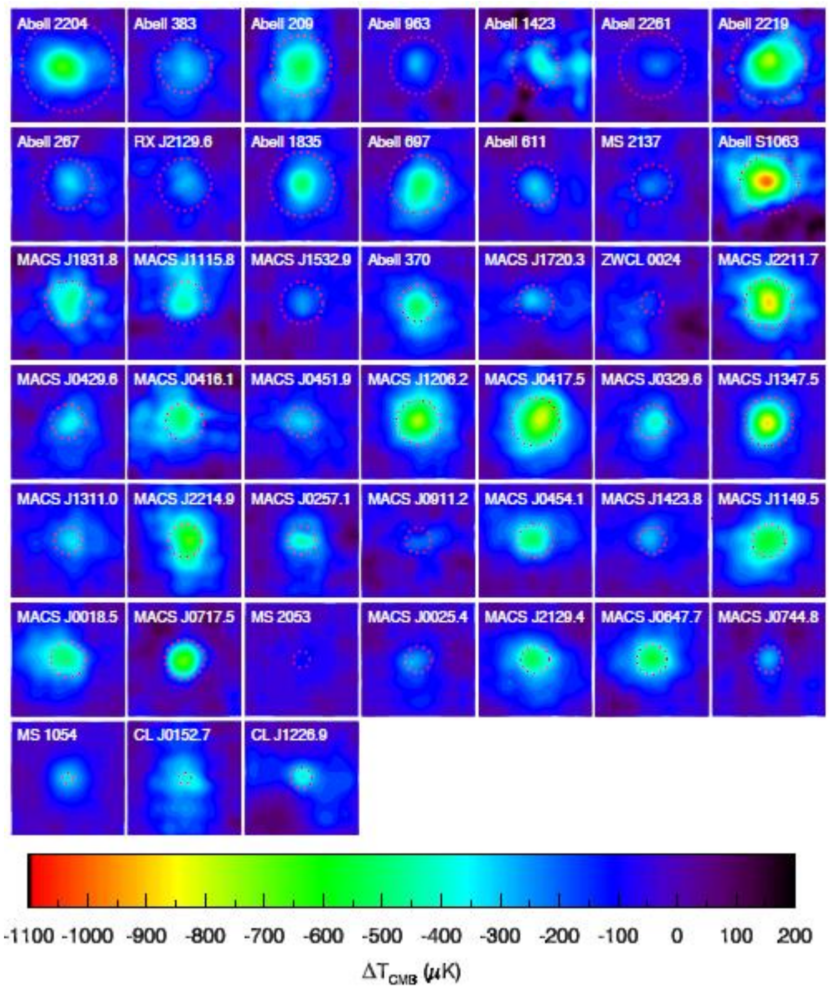

Wide-field SZE imaging with sub-arcmin resolution is ALSO sensitive to 2D gas-halo morphology:

- Bolocam/CSO with 58” (30”) PSF @ 150 (248) GHz, 14-arcmin map FoV
- MUSIC/CSO (2014~) will have about *x2* wider effective FoV
- Multiscale synthesis of interferometric data with ALMA+ACA and CARMA will also be promising.

Consistent joint SZ+X modeling of 3D ICM structure is in progress by integrating Bolocam data into JACO by CLASH+ collaboration (Mahdavi, Sieagel, Sayers, Donahue+)

(3) Ensemble-averaged thermal pressure vs. total mass profiles from stacked SZE and lensing analyses

Ensemble-averaged Pressure Profile around Clusters

- Testing self-similarity (scalability) and predicted radial profile shape P(r) of the averaged pressure profile (Suto, Sasaki, & Makino 98; Komatsu & Seljak 01; Nagai+07; Arnaud+10; Cavaliere, Lapi & Fusco-Femiano 11)
  - Empirical tests of ICM morphology dependence
  - Empirical tests of non-gravitational processes in cluster cores and outskirts ($>r_{500}$)
  - Comparison with the lensing-derived averaged mass profile for examining the degree of HSE

- Warm gas in cluster filaments and LSS, or 2-halo term (Fang, Kadota, & Takada 12)

Stacked Pressure Profile of BOXSZ Sample (Sayers+13)

BOXSZ (Bolocam SZ/X-ray) sample tSZE analysis:

- 45 high-mass clusters @ 0.15<z<0.89 with $\langle M_{500c} \rangle = 9\times10^{14} M_{sun}$ including 25 CLASH clusters.
- X-ray Chandra data for determining r_{500} and P_{500}
- X-ray Chandra data for morphology classification
- 17 cool-core and 16 disturbed clusters (2 CC-disturbed)
- Arnaud+10: 33 clusters at z<0.2, XMM (inner), simulations (outer)
- Planck12: 62 clusters at <z> = 0.15, XMM (inner), Planck SZE (outer)

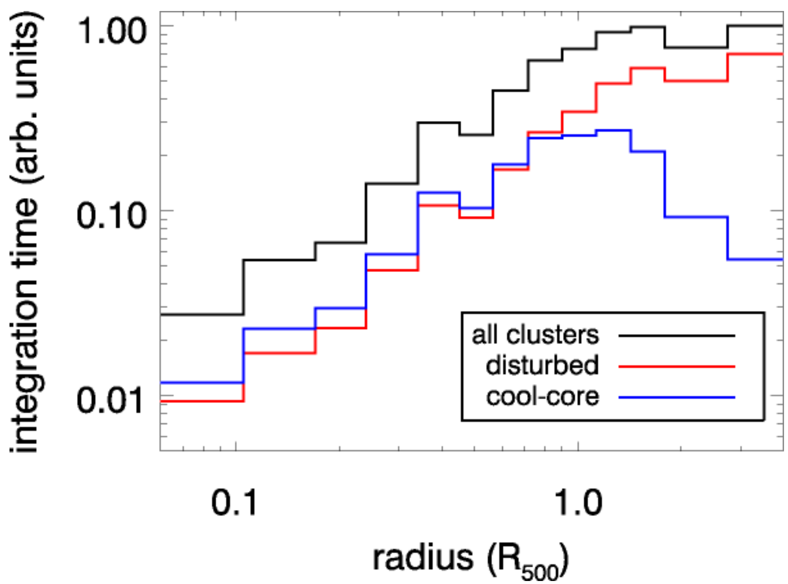

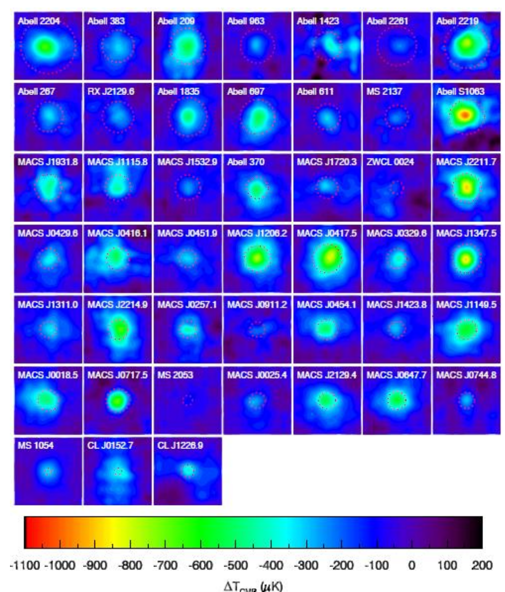

Stacked $P(R/R_{500})$ and gNFW fits

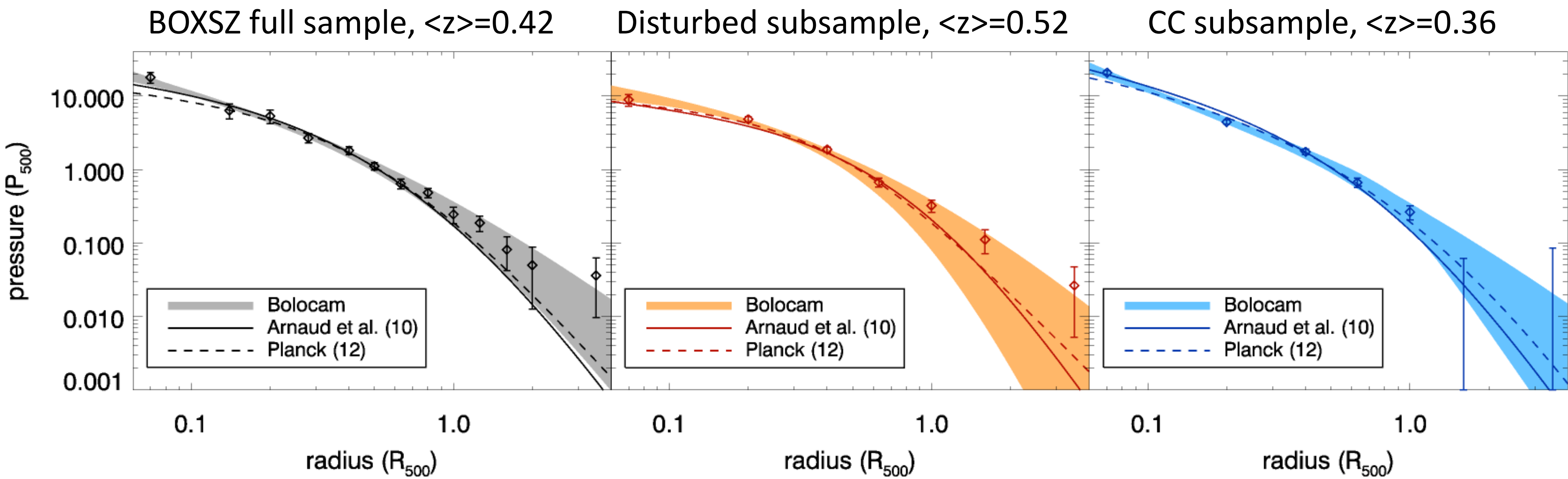

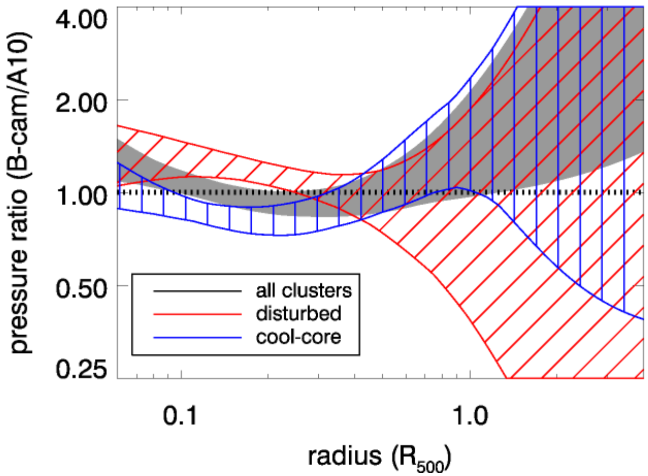

- gNFW gives a good fit to R = [0.07, 3.5]R_{500c}
- At r< 0.15 r_{500}, the CC clusters show higher pressures than the disturbed ones.
- Consistent pressure profiles at > 0.15 r_{500} between the CC and disturbed subsamples
- Consistent with other X/SZ results (Plagge+10; Melin+11; Planck 11; Komatsu+11).
- Hints of slightly higher pressures at the smallest and largest radii.

Sayers+13

Mean Pressure Profile and Intrinsic Scatter from Gaussian-Process Modeling

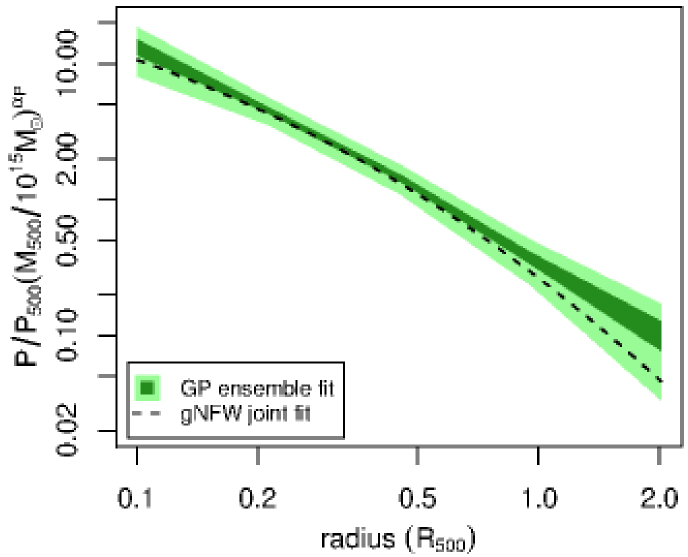

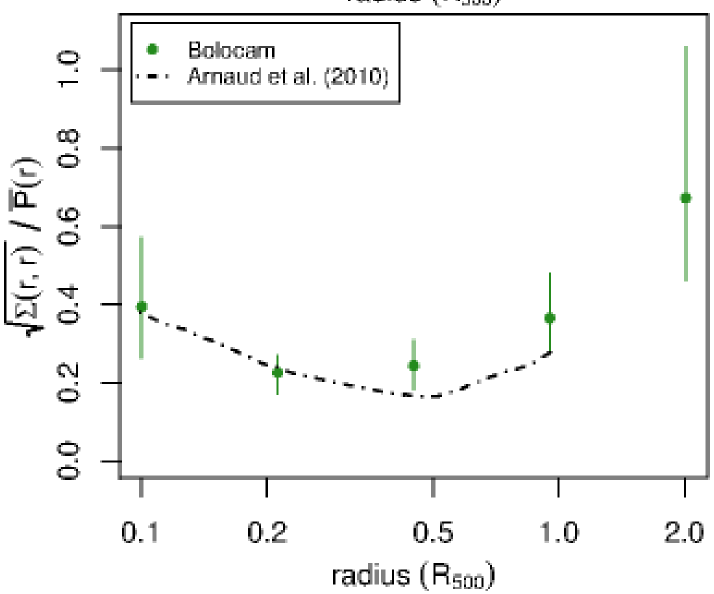

- Model individual cluster profiles as Gaussian process
  - simultaneously constrain mean profile, mass scaling, and intrinsic scatter
- Find mass scaling shallower than self-similar one
  - 0.49 compared to 2/3
- Intrinsic scatter minimized to ~20% at intermediate radii, ~0.5 R_{500c}

Sayers+13

Next Step

- Compare the stacked pressure and mass profiles for a statistical sample of clusters.
- Combining (1) SL, (2) WL-shear, and (3) WL-magnification allows us to derive the total projected mass profile $\Sigma(R)$ from R=10kpc/h to beyond R_{vir} (Umetsu+11b).
- CLASH lensing, SZE, and X-ray comparison

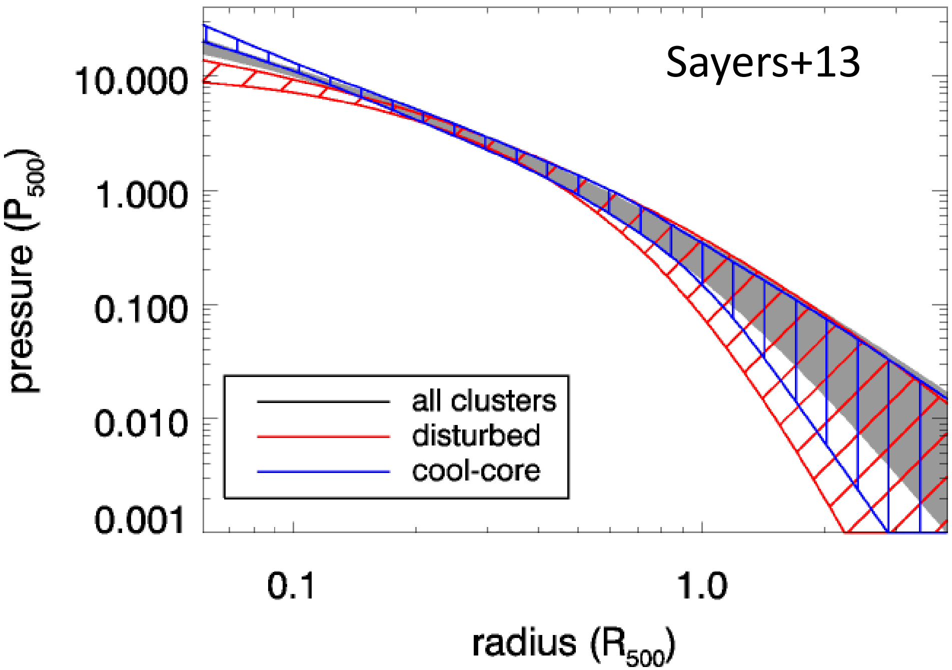

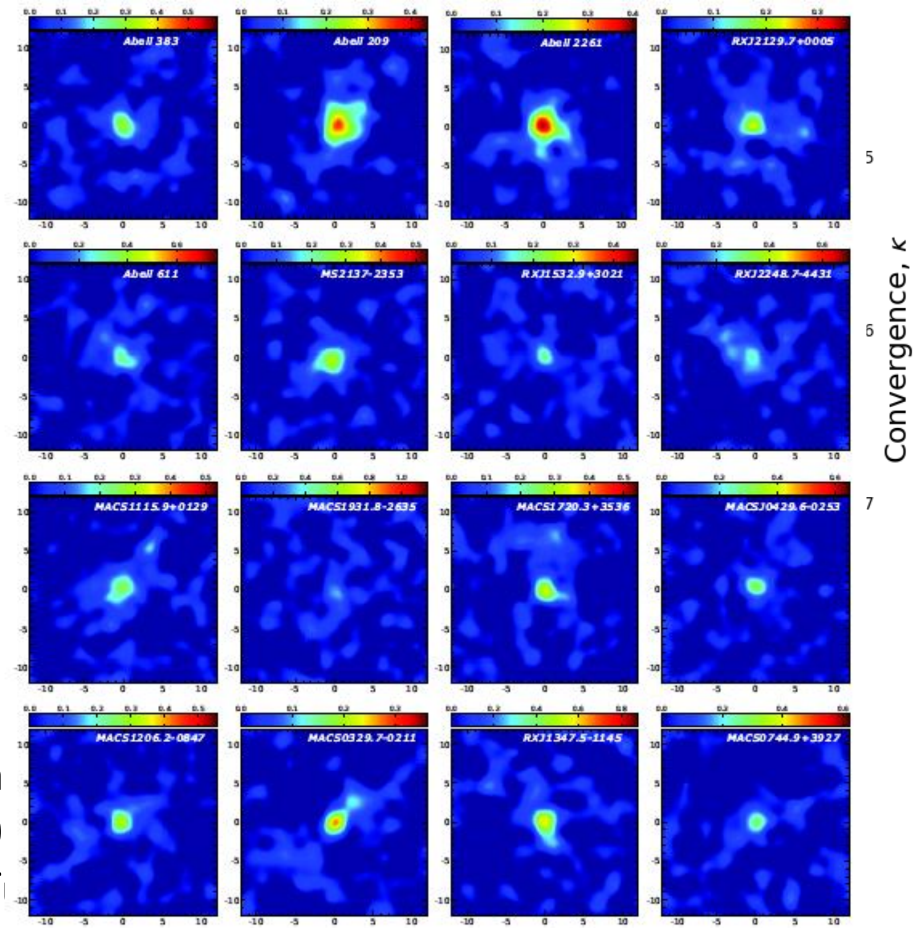

- Bolocam → MUSIC upgrade @CSO will im probing the radial range R = [0.07, 7]R500
- Subaru HSC-WL + ACT will be very powerf

Next Step

- Compare the stacked pressure and mass profiles for a statistical sample of clusters.
- Combining (1) SL, (2) WL-shear, and (3) WL-magnification allows us to derive the total projected mass profile Σ(R) from R=10kpc/h to beyond R_{vir} (Umetsu+11b).
- CLASH lensing, SZE, and X-ray comparison in progress.

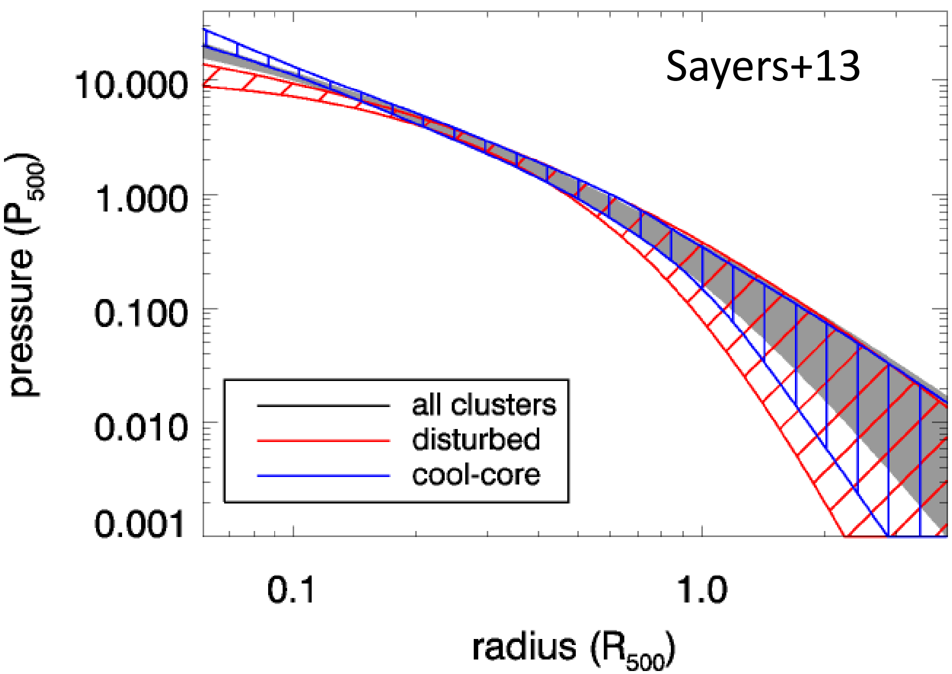

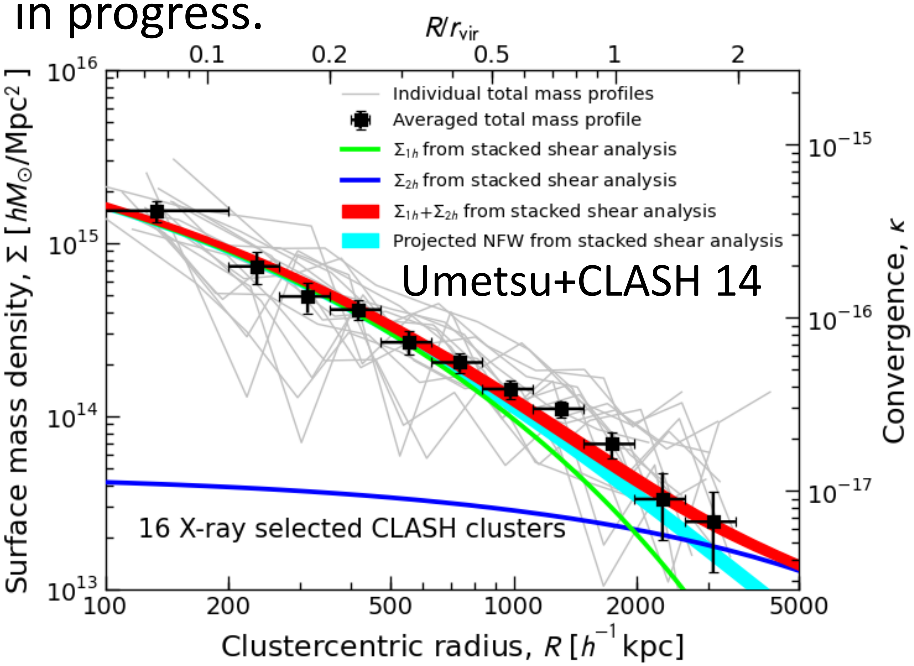

- Bolocam → MUSIC upgrade @CSO will improve the effective FoV by a factor of 2, probing the radial range R = [0.07, 7]R500 ~ [0.035, 3.5] R_{vir}
- Subaru HSC-WL + ACT will be very powerful for low-mass and high-z clusters.

Summary

- Multi-frequency high-resolution SZE + X-ray observations of moving substructures for LoS gas peculiar velocity measurements.
- ALMA and NIR (e.g., XSHOOTER on VLT) spectroscopy of multiply-lensed images in Bullet-like colliding clusters for tangential DM-peculiar-velocity measurements:
  - Large-separation multiply-lensed QSOs with many absorption feature (if any) are very useful because the errors get reduced by 1/sqrt[N]
  - For lensed galaxy images, once the source redshift is known, ALMA with high resolution is very powerful for measuring (narrow) molecular emission
- Spatially-resolved tSZE imaging with subarcmin-resolution and >10-arcmin-FoV can be used for multi-probe 3D cluster modeling of high-mass clusters (M_{500c}>5x$10^{14}$$M_{sun}$): Bolocam/MUSIC@CSO, ALMA+ACA, etc.
- Improved transfer function with CSO-to-MUSIC upgrade at CSO probing the stacked pressure profile out to $7R_{500c}$ ~ $3.5R_{vir}$ (?)
  - Still useful before CCAT replacement?

SZE instruments for pointed (targeted) observations

- Bolocam at CSO 10m
  - 140 GHz -> 8' FOV, 58” PSF, ~22μK_{CMB}-arcmin sensitivity
  - 268 GHz -> 31” PSF
  - MACS0717 at z=0.55: 3.3 mJy/beam@140 GHz, 1.8 mJy/beam@268 GHz (Sayers et al. 2013)
- MUSTANG at GBT 100m
  - 90 GHz -> 42” FOV, 10”-18” PSF
  - MACS0717 at z=0.55: 34 uJy/beam (Mroczkowski et al. 2012)
- CARMA/SZA interferometer array at Cedar Flat
  - An array of six 10m, nine 6m, eight 3.5m antennas at 30GHz and 90GHz
  - 12’ FOV, 0.3’ PSF (depending on config)
  - Follow up observations for SPT, XXM-XXL
- NIKA (KIDs based instrument) at IRAM 30m
  - 140 GHz, 132 pixels -> 1.8’ FOV, 18.5” PSF (see Adam+13, arXiv:1310.6237)
  - 240 GHz, 224 pixels -> 1.0’ FOV, 12.5” PSF
  - NIKA2 with 1000 and 4000 detectors at 140 and 240GHz (2015-)
- MUSIC at CSO 10m
  - 14’ FOV, 2304 detectors/ 576 spatial pixels
  - 0.86,1.0,1.3, & 2.0mm

Blue = under commissioning

WL vs. SZE morphology in A383

Subaru WL mass map
(Umetsu+CLASH 14, in prep)

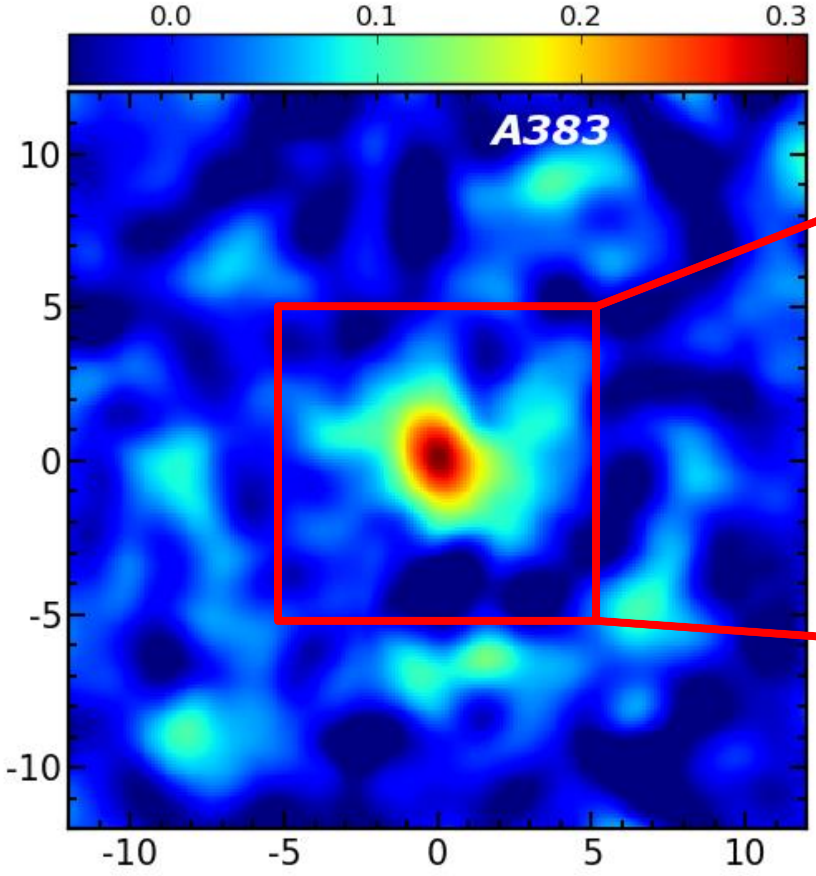

Bolocam SZE map@150GHz
(Zitrin et al. 2012)

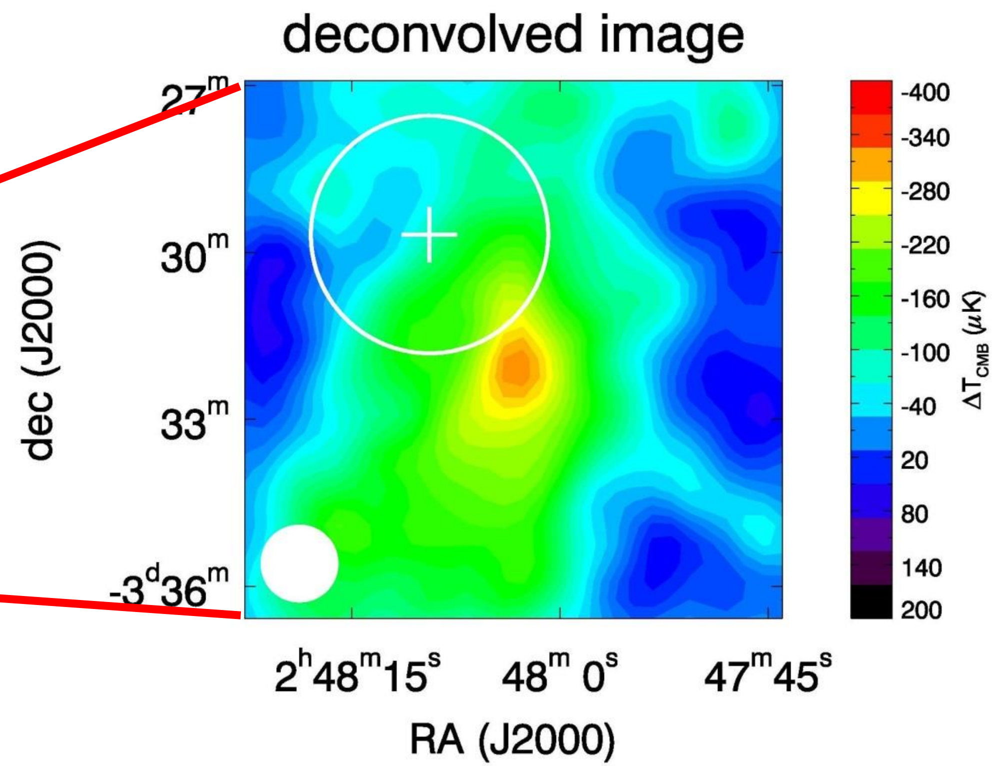

Averaged Lensing Profiles of LCDM Halos

Shear Doesn't See Mass Sheet

$\kappa = \Sigma / \Sigma_{\rm crit}$ $\gamma_T = \Delta\Sigma / \Sigma_{\rm crit}$

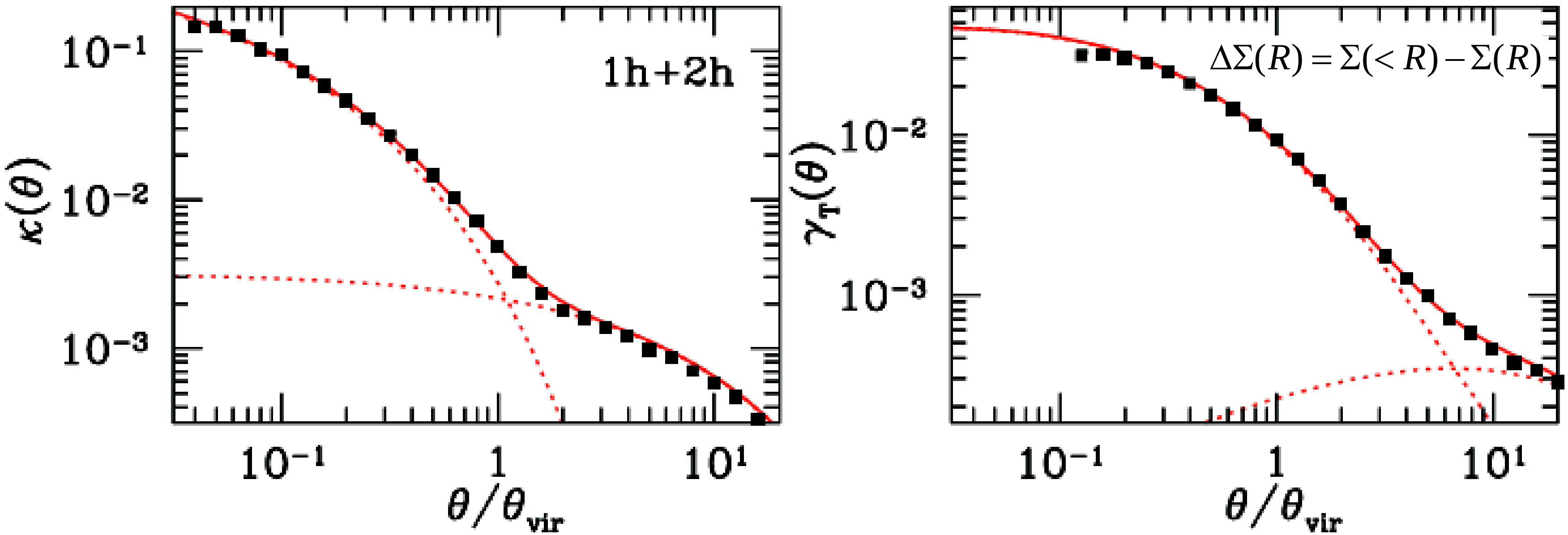

- Tangential shear is a powerful probe of **1-halo term**, **or internal halo structure**.
- Shear alone cannot recover absolute mass, known as ***mass-sheet degeneracy***.

Figures from Oguri & Hamana 11

CLASH X-ray-selected subsample

WL mass maps: 16 clusters completed

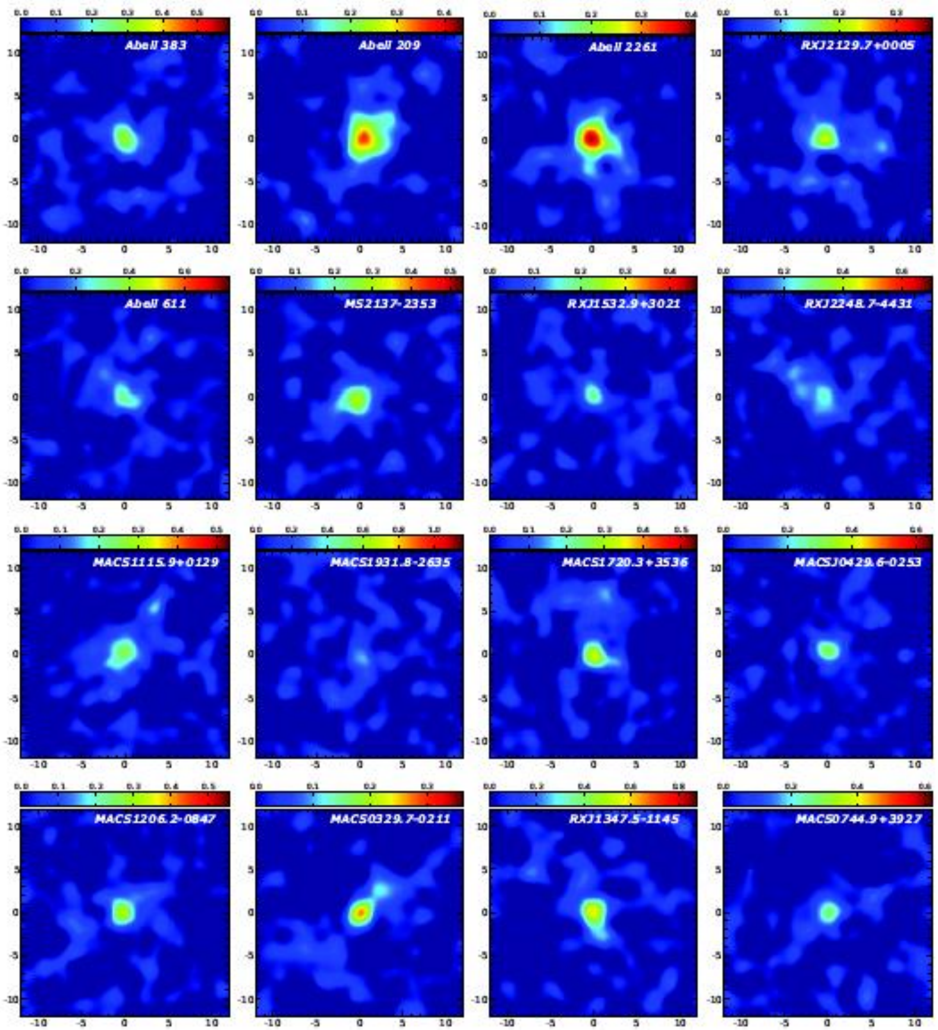

Umetsu+CLASH 14, in prep (Subaru, 24’x24’)

X-ray maps: 20 CLASH clusters are purely X-ray selected to be massive and relaxed

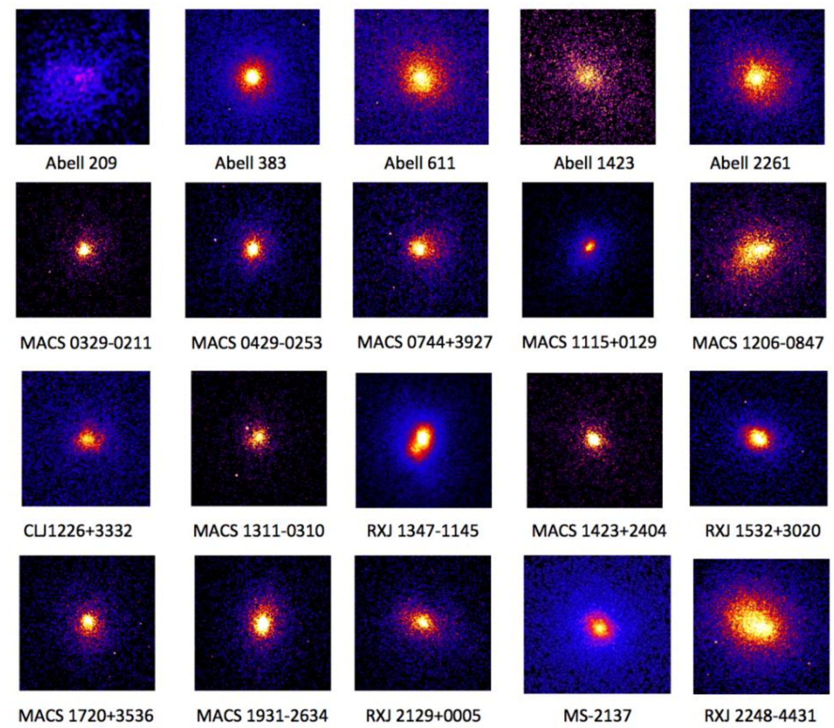

Postman+CLASH 12, ApJS

CLASH-WL: Stacked shear profile

Ensemble-averaged internal halo structure of X-ray-selected relaxed CLASH clusters with $\langle M_{200c} \rangle = 10^{15} M_{sun}/h$ at $\langle z \rangle = 0.35$

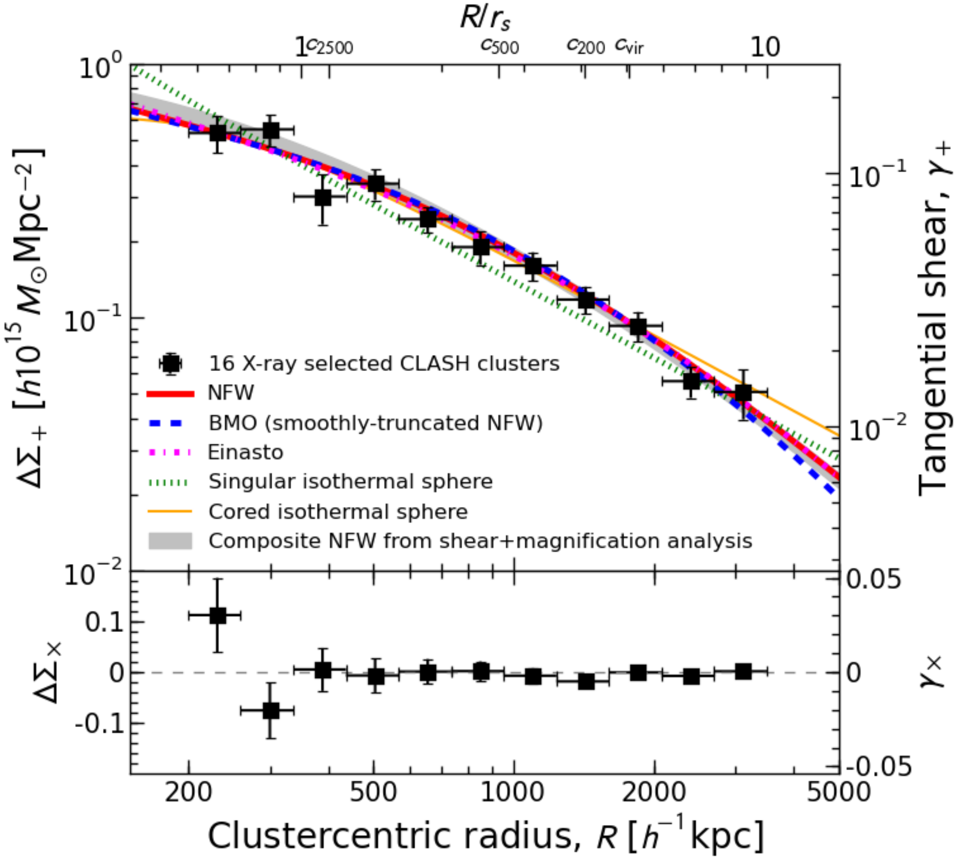

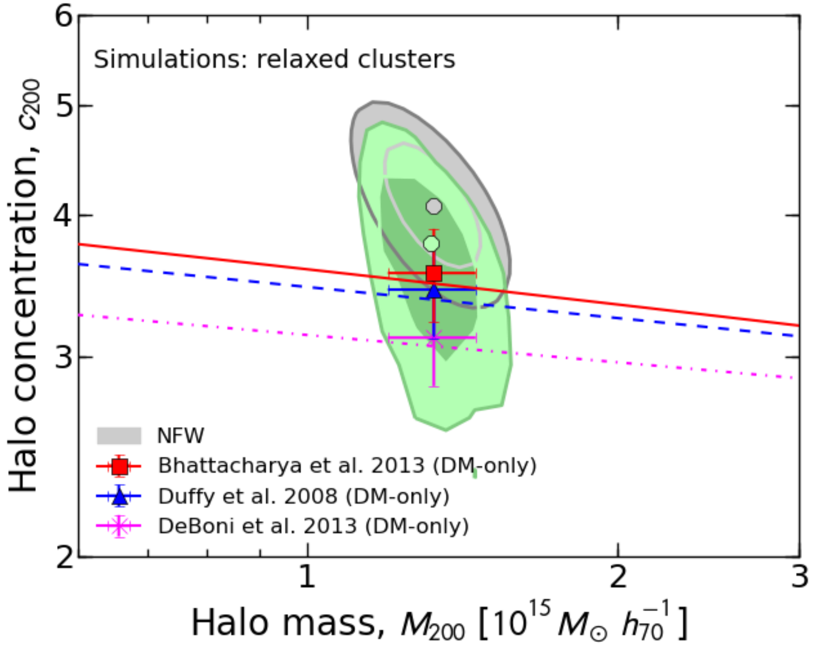

Umetsu+CLASH 14, in prep

Consistent with a family of density profiles for collisionless-DM halos in gravitational equilibrium (NFW, BMO, Einasto)

CLASH-WL: Stacked total mass profile from combined shear + magnification

- Measuring 1h+2h term out to $R=2r_{vir}$ around 16 X-ray clusters with $<M_{vir}>$=10e14Msun/h at $<z>$=0.35 → linear halo bias b_h= 9 (Tinker+10)
- Testing shear vs. magnification consistency in the context of LCDM

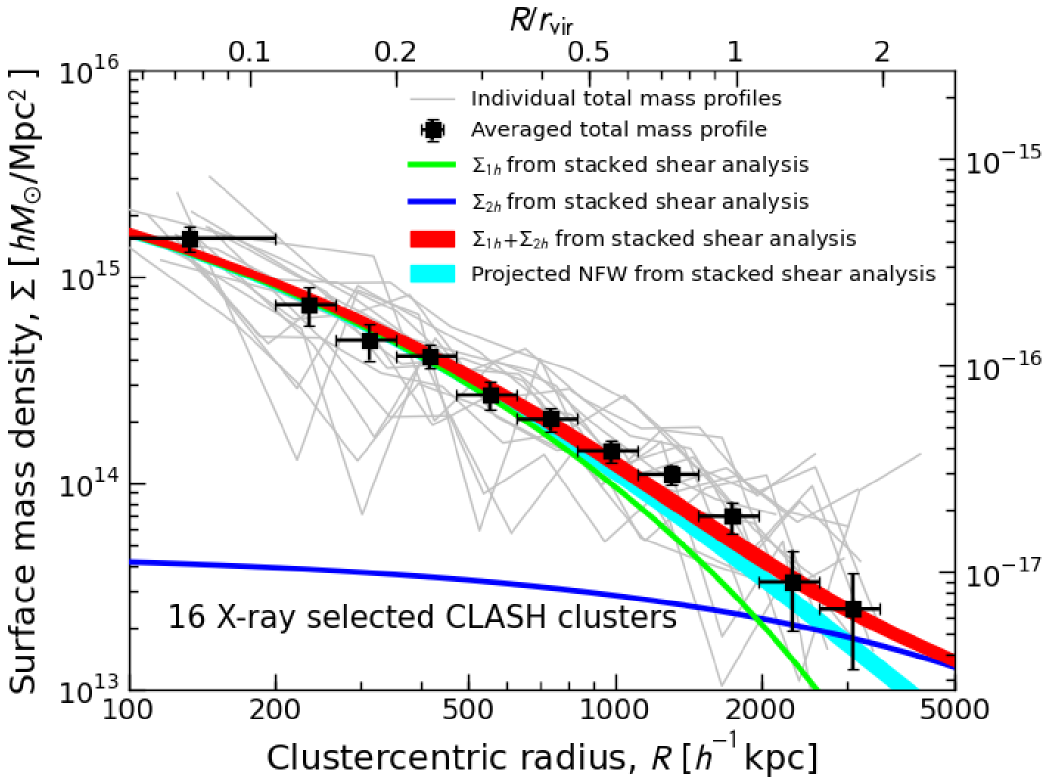

2D halo model decomposition:
smoothly-truncated NFW (BMO) + LCDM 2h-term

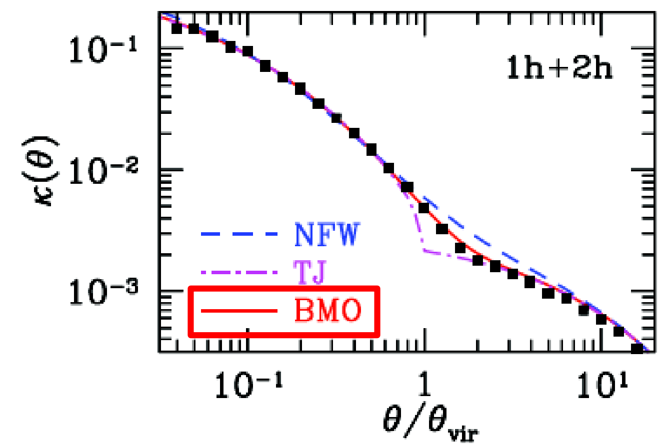

Umetsu+CLASH14 in prep

Strong-lensing, weak-lensing shear+magnifcation constraints on A1689

WL shear-magnification consistency
(Umetsu+11a Bayesian method)

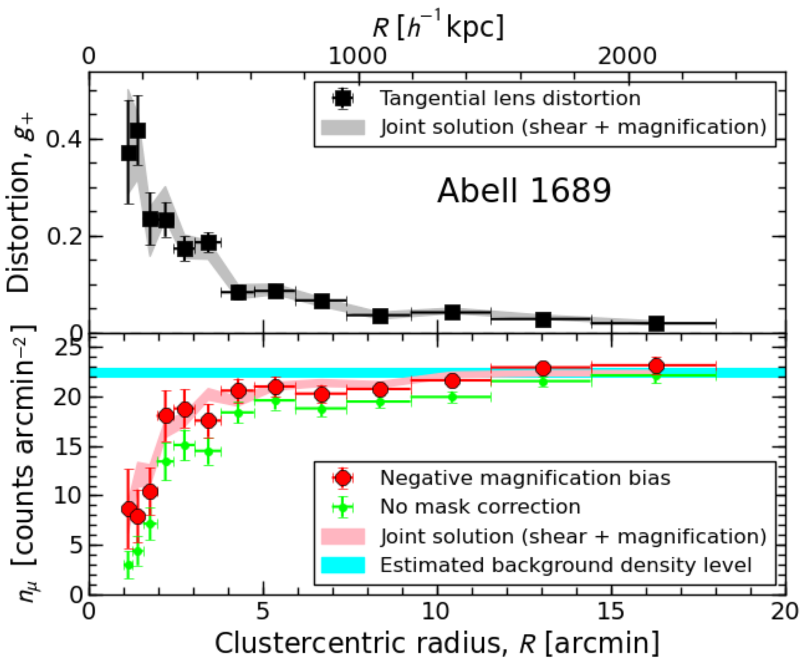

Strong-lensing vs. weak-lensing projected mass profiles

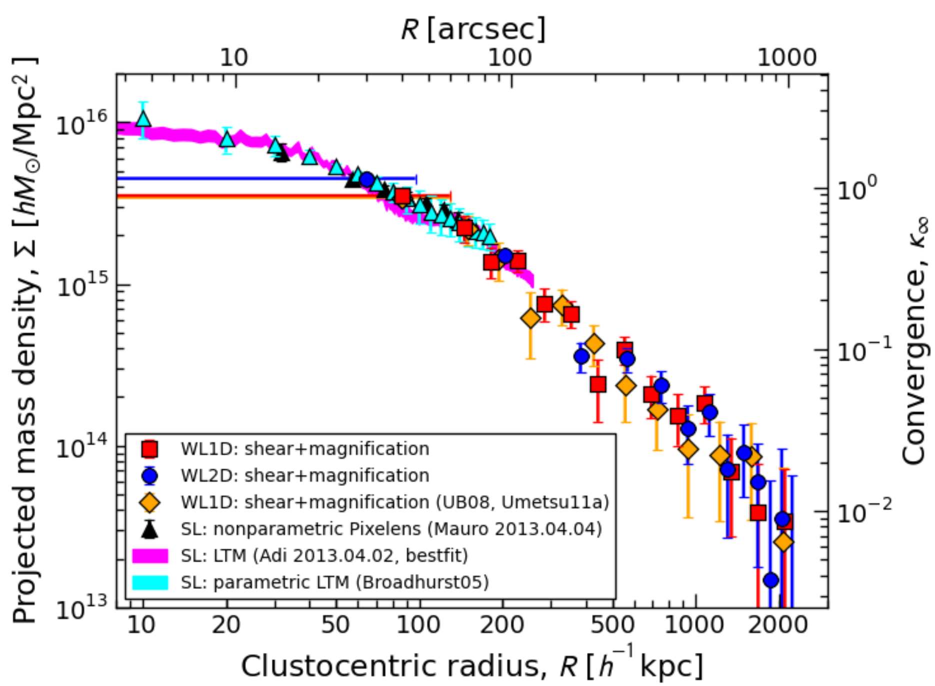

Projected total mass profile well described by the steepening NFW form